NOTE TO USERS

This reproduction is the best copy available.

UNIVERSITY OF CINCINNATI

February 27 , 2003

I, Richard Tyler Martin ,

hereby submit this as part of the requirements for the degree of:

Masters of Science

in Molecular and Developmental Biology

It is entitled The Role Hypoxia Plays During Embryonic Mouse Lung Development

Approved by:

James L. Lessard

Gary Weston

The Role Hypoxia Plays During Embryonic Mouse Lung Development

A thesis submitted to the

Division of Research and Advanced Studies
Of the University of Cincinnati

In partial fulfillment of the
requirements for the degree of

MASTER OF SCIENCE

in the Molecular and Developmental Biology Program
of the College of Medicine

2003

by

R Tyler Martin

B.S., Ball State University, 1999

Committee Chair: John M. Shannon, Ph.D.

Abstract

As the embryo reaches a critical size, oxygen can no longer diffuse to every cell, creating a hypoxic environment. A hypoxic environment is known to facilitate development of the Drosophila trachea, which is homologous to the mammalian lung. Embryonic mouse lung develops by branching morphogenesis but it is unknown if hypoxia plays a role. The goal of this project was to elucidate the role hypoxia might play during embryonic lung development. Hypoxia inducible factor 1 alpha (Hif-1-α), the regulated subunit from the HIF-1 transcription factor, exhibits dynamic expression during lung development. E11.5 and E13.5 lung explants cultured under hypoxic conditions exhibit an increase in gene expression, as well as differences in growth when compared to normoxic explants. Finally, triple transgenic mice in which Hif-1-α was deleted from the distal epithelium resulted in neonatal lethality. These data are consistent with the hypothesis that mouse lung development is effected by hypoxia.

Acknowledgements

I would like to acknowledge Dr. Randall Johnson (UCSD, San Diego, CA) and Dr. Jeffery Whitsett (CCHMC, Cincinnati, OH) for generously providing the transgenic mice used in this project.

I would like to acknowledge my mentor, Dr. John Shannon, for allowing me to work in his lab and providing me with an opportunity to be creative with this project. I would also like to acknowledge the Shannon lab for continuous support and direction during the experimental portion of this project.

I would like to acknowledge Dr. Jim Lessard and Dr. Ann Akeson for working on my thesis committee and for helping to point my research in the right direction.

I would like to acknowledge the program in Molecular and Developmental Biology for providing me with the opportunity to enhance the knowledge gained as an undergrad. I would like to thank Dr. Charles Vorhees and Dr. Dan Wiginton for providing sound and timely advice throughout my graduate education.

I would like to acknowledge Dr. Carl Warnes and the Ball State Biology department for helping me build a strong foundation in both the Biological and Laboratory sciences.

I would like to thank my family and friends for providing kind places to go to and relax and for the non-science related conversation in between the constant studying. Family has always been a great source for inspiration.

Last, but definitely not least, I would like to thank my wife, Emily, for being a constant positive influence from the first day we met. I couldn't have accomplished all that I have without her (in return, I have promised her a house on the coast).

Table of Contents

List of Figures

List of Symbols and Abbreviations

ug	Microgram
ul	Microliter
ml	Mililiter
mM	Milimolar
bHLH	Basic helix-loop-helix
bp	base pairs
Brdu	Bromeated uridine
C	degrees Celsius
cDNA	copy deoxyribonucleic acid
cd	culture day
DMEM	Dulbecco's modified Eagle's medium
E	embryonic day
FBS	Fetal bovine Serum
FGF	Fibroblast growth factor
FGFR	Fibroblast growth factor receptor
HA	Heme Aglutenin
HSPG	Heparin Sulfate Proteoglycan
Hif	Hypoxia inducible factor
HBSS	Hanks Balanced Salt Solution

HRE	Hypoxic Response Element
mRNA	messenger ribonucleic acid
ODD	oxygen dependent domain
O2	Oxygen
PCR	Polymerase Chain Reaction
pn	post natal day
rtTA	reverse tetracycline transactivator
sec	seconds
SPC	Surfactant Protein C
U	units
VHL	von Hipple Lindau protein

Introduction

The lung develops as a complex organ with epithelial, mesenchymal, and vascular compartments whose functions are integrated to facilitate gas exchange from air to blood, which is an essential process required to sustain normal mammalian respiration. Lung development begins in the mouse on embryonic day (E) 9.5 and continues until approximately postnatal day (pn) 14, encompassing a total of 33 days (Wessels, 70). During the early part of lung development, a simple epithelial out pouching from the ventral foregut endoderm undergoes a process of growth and repetitive branching. This process, referred to as branching morphogenesis, is driven by epithelial interactions with its surrounding mesenchyme, and is completed by E16 (Hilfer, 96). The developing lung must first complete pulmonary tree formation in order to become a functional organ.

Formation of the pulmonary tree lays the pattern for fine terminal branching, thus increasing the surface area for gas exchange (Taderera, 67). Tissue interactions drive this process, with the epithelium receiving instructions from the surrounding mesenchyme.

The nature of epithelial-mesenchymal interactions in the developing mouse lung was first studied using tissue culture techniques. Mouse lung was

found to be ideal for culture studies due to its ability to recapitulate *in vivo* branching morphogenesis in an *in vitro* environment (Spooner, 70). Shortly thereafter, techniques for the separation of lung epithelium and mesenchyme were developed, which allowed the development of transfilter and tissue recombination assays (Spooner, 70; Wessels, 70).

Transfilter recombinations make it possible to culture two separated tissues without contact while allowing the free passage of molecules through it. When embryonic lung epithelium and mesenchyme were cultured in this manner, epithelial buds formed and branched (Spooner, 70). This led to the conclusion that soluble factor, not cell-cell contact, initiate and sustain branching morphogenesis.

Tissue recombination experiments shed further light on the specifics of mesenchyme-epithelium interactions. If E11 mouse gut endoderm was recombined with E11 non-lung mesenchyme and cultured, epithelial buds formed but branching morphogenesis did not occur (Wessels, 70). If the same experiment was performed utilizing lung mesenchyme, epithelial buds formed and branching morphogenesis ensued (Wessels, 70). More specific recombination experiments followed in which lung and tracheal epithelium both budded and branched when recombined with lung mesenchyme, while tracheal mesenchyme inhibited these processes (Wessels, 70). Finally, it

was found that the degree to which lung epithelium would develop was dependent upon the mass of lung mesenchyme used for recombinations (Masters, 76). From these experiments, it was concluded that lung mesenchyme produces the factors necessary to instruct lung epithelium throughout the process of branching morphogenesis.

The molecular mechanisms controlling branching morphogenesis have been shown to be very complex. One family of molecules that play a central role is the fibroblast growth factors (FGF's). Homology based PCR revealed a novel member of the FGF family that was found to be highly homologous to FGF7 (Yamasaki, 96). This novel FGF, FGF10, was found highly expressed in rat and mouse lungs (Yamasaki, 98; Beer, 97). Spatial and temporal expression studies revealed FGF10 mRNA to be localized in mesenchyme adjacent to distal epithelium in whole mouse lung explants from E9.5 through 12.5 (Bellusci, 97). Collectively, these data suggest that FGF10 mRNA is expressed in the correct place and at the proper time to play a role in branching morphogenesis.

Functional assays were performed to shed light on the biological roles of FGF10. Transfection of human 293 cells with a HA tagged mouse FGF10 expression vector revealed the protein product to be in cell lysates, but not in the medium (Beers, 97). This was a curious result since the

protein was found to contain a signal peptide sequence that directs secretion from the cell that translates it (Yamasaki, 96). A possible explanation for these observations is the primary sequence also contains two N-linked glycosylation sites that allow the protein to bind heparin sulfate proteoglycan (HSPG) components of either the cell surface or the extracellular matrix (Beer, 97). Addition of heparin, which competes with FGF's for binding both extracellular matrix and cell surface HPSG, caused FGF10 to be released into the surrounding medium (Beer, 97; Ornitz, 00).

Recombinant protein and targeted gene deletion technology helped identify FGF10's specific role during lung development in vivo. Embryonic day 11.5 mouse lung distal epithelium denuded of its mesenchyme formed buds when treated with recombinant FGF10 in culture (Bellusci, 97). FGF10 released from a heparin-coated bead that was placed proximal to embryonic mouse distal lung epithelium elicited growth toward the protein source (Park, 98). Further studies combining epithelial growth with Brdu uptake (a marker of DNA synthesis) revealed that FGF10 was a modest proliferation factor (Park, 98). Finally, a mouse model was created in which the FGF10 locus was targeted for inactivation. While embryonic lethality did not occur, the lack of FGF10 resulted in a complete lack of lungs and limbs, resulting in neonatal death (Min, 98).

Prior to the discovery of FGF10, it was already known that the response to FGF is to mediate a response through high affinity tyrosine kinase receptors. There are four known major classes of FGF receptors, FGFR1 through 4 (Powers, 00), and all four have been found localized to the lung (Powers, 00). FGFR1 and 2 are found on the surface of mesenchymal and epithelial cells of the developing lung rudiments (Peters, 92). More specifically, the FGFR2IIIb and 2IIIc splice isoforms are found on the surface of lung epithelial and mesenchymal cells, respectively (Arman, 99). FGFR2 knockouts resulted in early embryonic lethality by E10, just prior to organ development (Xu, 98). By using chimeric protein expression technology, a mouse was engineered in which FGFR2 could be mutated just prior to organ development (Arman, 99). The resulting phenotype was the absence of lung development, similar to the FGF10 -/- mice (Arman, 99). Shortly thereafter, a transgenic mouse was created in order to determine which FGFR2 splice isoform was responsible for the mutant lung phenotype. If FGFR2IIIb splice isoform was specifically deleted prior to organ development, lungs failed to form (Dermerlooze, 00). These results supported data found via ligand binding assays in which FGF10 was found to preferentially bind the FGFR2IIIb splice isoform (Celli, 99).

The data produced from both the FGF10 and FGFR2IIIb experiments suggest the way in which epithelium and mesenchyme interact during lung branching morphogenesis. FGF10 is expressed, translated, and processed for secretion from lung mesenchymal cells adjacent to the distal epithelium. The FGF10 ligand binds to the FGFR2IIIb isoform found on the surface of the distal lung epithelium. Upon binding its receptor, FGF10 elicits a response from FGFR2IIIb in the form of a signal transduction cascade within the targeted epithelial cells (Powers, 00). The signal transduction cascade results in distal epithelial cell growth and migration towards the source of the FGF10 ligand.

Drosophila tracheal development occurs in much the same way as mammalian lung. The Drosophila trachea is a branching epithelial mass that migrates in a receptor-ligand-mediated fashion. The receptor and ligand that facilitates tracheal branching is homologous to the receptor and ligand combination that directs branching morphogenesis in the developing mammalian lung (Metzger, 99). The Breathless receptor, which is homologous to mammalian FGFR, is found ubiquitously on the surface of the developing trachea (Klambt, 92). The tissue surrounding the advancing tracheal branches secretes Branchless FGF, which is homologous to mammalian FGF10 (Sutherland, 96). Branchless secretion guides the

direction in which the trachea will migrate by binding and activating the breathless receptor (Jarecki, 99).

Branching of the Drosophila trachea during development is controlled by both molecular and physiological cues. Branchless expression is regulated in specific regions of the larva by O2 tension(Jarecki, 99). Once the larva reaches a critical size, regions of low O2 tension (hypoxia) are created (Jarecki, 99). Hypoxia triggers the expression of Branchless (Jarecki, 99). Breathless FGFR expression is controlled by the Trachealess/Tango bHLH transcription factor (Ohshiro, 97). Although the Breathless receptor is expressed ubiquitously on the surface of the developing trachea, it is activated only where its ligand is located. This sets up a scenario in which hypoxia dictates where the trachea will branch and migrate (Ohshiro, 02).

Although it is known that hypoxia dictates where the Drosophila trachea will branch and migrate, it is not known if mammalian lung development is influenced in the same manner. It is known that the developing mammalian embryo becomes hypoxic once it reaches a critical size in which O2 cannot diffuse to all tissue areas (Semenza, 99). The Breathless and Branchless program is homologous to what the mammalian lung uses for branching morphogenesis, i.e. FGF10 and FGFR2IIIb (Jarecki,

99). Trachealess and Tango, which activate expression of the Breathless FGFR in Drosophila, are homologous to mammalian hypoxia inducible factor (Hif)-1-α and Hif-1-β, respectively (Jarecki, 99). Hif-1-α/β heterodimer, otherwise known as HIF-1 transcription factor, is the molecular modulator of cellular hypoxia (Zhu, 96). What is not known, however, is if HIF-1 and/or hypoxia play any role during mammalian lung development.

Hypoxia is a physiological state in which atmospheric O2 falls below 90mmHg. Hypoxia can be categorized based upon the duration of low oxygen tension. Acute hypoxia lasts seconds to minutes and results in post translational modification of proteins (Semenza, 99). Chronic hypoxia lasts minutes to hours, and results in changes in gene expression (Semenza, 99). Some genes affected by chronic hypoxia are involved in the glycolytic pathway, vasculogenic and vascular remodeling, and red blood cell production (Zhu, 99; Semenza, 00).

All nucleated eukaryotic cells have the capacity to sense and respond to low oxygen tension (Semenza, 00). Although a consensus cellular oxygen sensor has not yet been identified, several putative structures have been proposed. Evidence exists that a NAD(P)H oxidase located in the plasma membrane of nucleated cells can relay the status of extracellular oxygen to the inside of the cell (Zhu, 99). Intracellularly, the oxygen signal is relayed

from the putative membrane bound sensor to the HIF-1 transcription factor via a prolyl hydrolase (Bruick, 01). When oxygen levels are high, the prolyl hydrolase hydroxylates proline 564 of the Hif-1-α subunit of the HIF-1 transcription factor (Jaakkola, 01). The hydroxylated Hif-1-α subunit is thereby tagged for recognition by the von Hipple-Lindau (VHL) protein (Ivan, 01). The VHL tagged Hif-1-α is then recognized and destroyed by the proteasomal degradation pathway (Ivan, 01). When cells experience hypoxia, prolyl hydroxylation does not occur, and hif-1-a is stabilized (Jaakkola, 01).

Stabilization of Hif-1-α allows it to immediately heterodimerize with Hif-1-β. Once the HIF-1 heterodimer is formed, the transcription factor is actively transported to the nucleus where it binds to target genes containing the 5'-RCGTG-3' hypoxia response element (HRE) (Semenza, 96). By binding the HRE, the HIF-1 transcription drives the expression of the target gene in an oxygen level dependent fashion (Zhu, 01).

Evidence from transgenic research demonstrates that HIF-1 transcription factor plays a role in embryonic development. Targeted deletion of HIF-1's regulated subunit, Hif-1-α, results in a lethal phenotype by E9.5 in the mouse (Kotch, 99). This result poses a problem for studying

the role of HIF-1 in embryonic lung development because the lung primordia do not evaginate from the foregut until day E9.5 (Perl, 99).

The goal of this project is to demonstrate the role that hypoxia plays during early mouse lung development. Specifically, this project will involve analyzing the regulated subunit, Hif-1-α, in several aspects of mouse lung development. We will first define the developmental profile for the temporal and spatial expression pattern of Hif-1-α mRNA, by evaluating Hif-1-α expression in the lung from E10.5 to postnatal day (pn) 1. Second, we will determine the effects a hypoxic environment has on the morphogenesis of cultured embryonic lung explants, and will define changes in several genes involved in lung morphogenesis and differentiation. The lungs cultured under hypoxic conditions will be compared to lungs cultured under normoxic conditions. Finally, we use a triple transgenic system in which Cre recombinase is conditionally expressed in the distal lung epithelium to delete Hif-1-α. This will enable us to define the importance of epithelial Hif-1-α to normal lung development. The advantage of the conditional gene knockout experiment is that it circumvents the embryonic lethality that is observed just prior to lung development in Hif-1-α knockout mice (Kotch, 99).

Methods and Materials

Mouse Embryos: FVBN males and females (Taconic Farms, Inc., Germantown, NY) were mated overnight and plugs were checked the following morning as an indicator of conception. Plug day was designated embryonic day (E) 0.5. Pregnant dams were sacrificed by C02 inhalation, and the uterine horns were removed on days E10.5 through 18.5 as dictated by the specific experiment. Uterine horns were placed immediately into ice-cold Hanks balanced salt solution (HBSS). Embryos were removed from the uterine horn and placed in ice cold HBSS.

Embryonic lung dissection and culture: Lungs were dissected from time dated embryos utilizing Moria microsurgery knives (Fine Science Tools, Foster City, CA) and placed immediately into ice cold HBSS. All dissections were performed using a Nikon SMZ-U dissecting microscope. Dissected lungs were placed on a semisolid medium in DMEM/F12 medium containing 0.5% agarose plus 5% FBS (GIBCO, Carlsbad, CA). The DMEM/F12 medium was supplemented with 100U/ml penicillin, 100ug/ml streptomycin, 100ug/ml glutamine, and 5% FBS (GIBCO, Carlsbad, CA). All medium used for culture was pre-equilibriated in either 21% or 3% 02 for 24 hours at 37•C prior to use. Dissected lungs were cultured for 3 days

under the same conditions used for pre-equilibriating DMEM. Specimens were photographed using an Olympus D10 digital camera.

RNA Isolation: Total RNA was isolated from cultured and uncultured embryonic mouse lungs utilizing the Eppendorf Phase Lock Gel protocol with small changes. Briefly, dissected lungs were placed into 1.5 ml Eppendorf tubes, then 200 uL GITC was added and the tissue was hand homogenized. Total RNA was isolated using the acidified guanidine procedure (Chomczynski, 1987). The isolated RNA was treated with DNaseI (DNA free kit, Ambion, Austin, TX) to remove any contaminating genomic DNA.

cDNA Synthesis: 1 ug of total RNA was converted to cDNA utilizing the cDNA Cycle Kit (Invitrogen, Carlsbad, CA) protocol with the change that, prior to precipitation, the cDNA was treated with 2U/ul ribonuclease H (Invitrogen, Carlsbad, CA). cDNA was extracted with Phenol:Chloroform:Isoamyl alcohol (25:24:1), then precipitated overnight in 2.5X volume 100% EtOH and 1/10 volume 7.5mM ammonium acetate - 70°C.

Real-Time PCR Analysis: Isolated cDNAs were analyzed for quantitative expression of specific genes using real-time PCR (Smart Cycler, Cephied, Sunnyvale, CA). Total RNA was isolated and reverse transcription

was performed on each sample as described above. Each gene was analyzed utilizing the same general parameters: 95°C for 125 sec., followed by 40 cycles of amplification (95°C for 12 sec., ~56-60°C for 14 sec., and 72°C for 12 sec.). Reaction conditions called for 10μM forward and reverse primers, 2.5mM MgCl2, and 1X DNA Master SYBR Green (Roche Molecular Biochemicals, Indianapolis, IN) which contains dNTP, Taq polymerase, buffer and SYBR Green dye. Forward and reverse primers (Invitrogen) designed to target specific genes were as follows:

β-actin (350bp) 5'-TGGAATCCTGTGGCATCCATGAAAC-3', 5'-TAAAAC GCAGCTCAGT AACAGTCCG-3';

Hif-1-α (182bp) 5'-ACAACTGCCAC CACTGATGAATC-3', 5'-ATGACTCTCTTTCCTGCTCTGTCTG-3';

Hif-2-α (132bp) 5'-TGGTAGAACTCATAGGCAGAGGCG-3', 5'-CCTGGAC AGCAAG ACTTTCCTG-3';

Fgf-10 (210bp) 5'-TGTCTT CGTTCC CTGTCACCTG-3', 5'-CCTTGCCGTTCTTCTCAATCG-3';

Fgf7 (108bp) 5'-AGCAAA GGGCTACGAGTGTGAAC-3', 5'-TGGGTGCGA CAGAACAG TCTTC-3';

FgfR2IIIb (162bp) 5'-AAGGTTTACAGCGATGCCCAG-3', 5'-CTCCGTCACATTGAACAGAGCC-3'.

Conditional deletion of Hif-1-α from the lung epithelium: Mice in which the Hif-1-α locus was flanked by lox P sites were obtained as a generous gift from Dr. Randall Johnson, UCSD, San Diego, CA. Two additional transgenic mouse strains were provided as a generous gift from Jeffery Whitsett, CCHMC, Cincinnati, OH. The first strain (SPC/rtTA) is one in which the 3.7 kb human SPC promoter drives expression of the reverse tetracycline response transactivator (rtTA). The second strain (otet/Cre) is one that contains a chimeric transgene consisting of seven copies of the tetracycline operator, a minimal cytomegalovirus (CMV) promoter, and Cre recombinase. All transgenic mouse lines were kept in a germ free barrier facility, CCHMC, Cincinnati, OH. A breeding strategy was designed that led to a final mating which produced transgenic pups in which Hif-1-α would be deleted (floxed out) from lung epithelial cells (Figure 10). SPC rtTA +/-, Hif floxed +/+, and CRE recombinase +/+ mice were crossed with SPCrtTA -/-, Hif floxed +/+, CRE recombinase +/+ mice. Plugs were checked every morning with a positive plug date equaling E0.5. Pregnant dams were fed doxycycline beginning on E3 of their pregnancy and continued until DOB. All mice involved in study were PCR genotyped for transgenes with the following primers (Invitrogen):

SPC rtTA (280bp) 5'-GACACATATAAGA CCCTGGTCA-3', 5'-AAAATCTTGCCAGCTTTCCCC-3';

CRE recombinase (374bp) 5'-TGCCACGACCA AGTGACAG CAATG-3', 5'-AGAGACGGAAATCCATCGCTCG-3';

Floxed Hif-1-a (250bp for wild type allele, 300bp for floxed allele) 5'-GCAGTTAAGAGCACTAGTTG-3', 5'-GGAGTATCTCTCTAGACC-3'. Reaction conditions were the same for all three primers used: 10X PCR buffer (Roche), 10μM forward and reverse primers, 10mm dNTP (Roche) mixed, and 1 unit of Taq polymerase (Roche). Reagents were brought to a final volume of 50μl with ddH_2O. DNA isolation from transgenic mouse tissue was done utilizing a protocol developed in the Whitsett Lab, CCHMC, Cincinnati, OH. 300ng total DNA was used for genotyping and the following PCR conditions were used for each primer: 95°C for 5 min; 95°C for 20 sec, 60°C for 20 sec and 72°C for 20 sec for 35 cycles; 72°C for 4 min. Gel electrophoresis analysis was performed in order to view a band indicative of PCR amplification.

Lung histology was performed according to protocols used by the Morphology Core in the Pulmonary division at Cincinnati Children's Hospital Medical Center.

Results

Expression of FGF10, FGF7, FGFR2IIIb, Hif-1-α and Hif-2-α in the Developing Lung: The results from the developmental profile revealed several interesting concepts that involve gene expression from one embryonic day to another. First, expression of FGF10, 7 and FGFR2IIIb was found to be dynamic over the course of lung development (Figure 4A). Compared to the expression levels in ED10.5 lung, FGF10, FGF7 and FGFR2/IIIb expression peaked on ED16.5. These genes then returned to a baseline expression level by adulthood. Second, both hif-1-α and Hif-2-α gene expression was dynamic over time (Figure 4B). The hypoxic response gene, Hif-1-α, peaked on ED16.5 while its homolog, Hif-2-α, showed a transient decrease in expression on ED16.5 (Figure 4B). Third, of all the genes examined, only Hif-2-α gene expression increased dramatically after ED16.5 (Figure 4B).

Effects of Hypoxia growth of E11.5 Lung explants In Culture: The results from culturing E11.5 lungs in hypoxic or normoxic oxygen conditions revealed some morphological differences. Lung explants cultured under hypoxic conditions appeared to undergo a thickening of mesenchyme as early as culture day (cd) 1 compared to those explants

cultured under normoxic conditions (Figure 5B2 and 5A2, respectively). Also, epithelial branches were smaller in hypoxic culture conditions compared to cd1 explants cultured under normoxic conditions (Figure 5B2 and 5A2, respectively). By cd2, the hypoxic lung explants appear to take on a more 3-dimensional appearance when compared to the normoxic lung explants (figure 5B3 and 5A3, respectively). By cd3, the normoxic lung explant epithelial branches become dimensionally similar to those of the hypoxic explants (Figure 5A4 and 5B4, respectively). The hypoxic explants took on an even greater 3-D appearance by cd3 (Figure 5B4) while the normoxic lung explant flattened out (Figure 5A4).

Effects of Hypoxia on Gene Expression in Cultured E11.5 Lung explants: The results from gene expression profiling E11.5 lung explants is shown on Figure 5. Results for the four gene expression profiles were compared to uncultured E11.5 lungs (cd0). Figure 6A reveals an 80% increase in FGF10 gene expression in lung explants cultured under hypoxic conditions for 3 days (cd3 H) while FGF10 expression increases 40% under normoxic conditions (cd3 NH). Figure 6B reveals a 190% increase in FGFR2/IIIb gene expression in cd3 hypoxic explants while cd3 normoxic explants showed a 140% increase. Figure 6C shows that Hif-1-α gene expression did not change cd3 hypoxic explants, while expression in

normoxic expression increased 30%. Examination of Hif-2-α expression (Figure 6D) revealed a minimal decrease (10%) in cd3 hypoxic explants, while normoxic explants exhibited a minimal (10%)increase.

Effects of Hypoxia on Growth of E13.5 Lung Explants: The same experiment performed on lung explants shown in figure 5 was repeated, except that E13.5 lung explants were used as starting material. The most striking results from these experiments were that the hypoxic lung explants exhibited epithelial branches that were larger in size than the normoxic cultures after 2 days (Figure 7A3 and B3). Furthermore, the mesenchyme from the normoxic explants on cd2 was thicker than the cd2 hypoxic explants (Figure 7A3 and 7B3). These results are the opposite of those found in the ED11.5 explant culture experiments (compare figure 5A2 and B2 with 7A3 and B2). Finally, cd3 hypoxic explants appear to have more epithelial branches when compared to cd3 normoxic lung explants (Figure 7B4 and 7A4, respectively). In contrast to E11.5 hypoxic lung explants, both ED13.5 hypoxic and normoxic lung explants flatten out by cd3 (compare figure 5A4 and B4 with figure 7A4 and B4).

Effects of Hypoxia on Gene Expression in Cultured E13.5 Lung Explants: Results from gene expression profiling in cultured ED13.5 lung

explants is shown in Figure 8. An interesting contrast in Hif-1-a and FGF10 gene expression exists between cd3 hypoxic explants and cd3 normoxic explants. Hif-1-α gene expression increases 90% in hypoxic lung explants as compared to 20% in normoxic lung explants (Figure 7a). Also, FGF10 expression increases 480% in hypoxic lung explants as compared to a 40% increase in normoxic lung explants (Figure 8b). All increases in gene expression are revealed when comparing E13.5 cd3 lungs to E13.5 cd0 controls.

Breeding Strategy Followed to Produce Triple Transgenic Mice: Figure 9 is a schematic that depicts a breeding plan used to arrive at the final triple transgenic product. The offspring from each breeding strategy were genotyped via Polymerase Chain Reaction (PCR). Breeding strategy #3 is performed using double transgenic mice created in breeding plan #1 and #2.

Schematic Representation of How Hif-1-α is Floxed from the Triple Transgenic Mouse Genome: Figure 10 shows how Hif-1-α is floxed from the triple transgenic mouse genome upon ingestion of doxycycline. The SPC promoter drives expression of the rtTA transgene. Whenever the SPC promoter is active, rtTA is expressed. SPC is expressed in the distal lung epithelium which means rtTA will only be expressed in that area. Doxycycline (dox), when ingested by the pregnant dam, circulates

throughout the body, entering virtually every cell type. When the dox enters a distal lung epithelial cell that has an active SPC promoter, it will complex with rtTA. This complex can now bind to the Otet octamer found on the promoter for the cre recombinase transgene. Binding of rtTA/dox to the Otet octamer initiates expression of cre recombinase. Wherever there is Hif-1-α flanked by flox sites and cre recombinase is expressed, recombination occurs and the flanked gene is deleted. This allows for the study of the effects that deleting Hif-1-α has on distal lung epithelium in both a temporal and spatial manner. This is very necessary technology when considering the fact that, when Hif-1-α is knocked out, embryonic lethality results as early as E9, which is when lung development begins (Kotch, 99).

Effects of Deleting Hif-1-α on Lung Development: In order to determine the role of Hif-1-α on lung development, we generated triple transgenic mice in which Hif-1-α was specifically deleted from the distal lung epithelium beginning by E10.. The results are shown in figures 11 and 12. Whole lungs dissected from either Hif-1-α positive or negative E14.5 embryos were photographed immediately following their removal (Figure 11 A and C, respectively). Branching morphogenesis did not appear to be affected by the deletion of Hif-1-α, nor were lung size or epithelial and mesenchyme proportions (Figure 11A + 11C). Sections of either Hif-1-α

positive (Figure 11B) or Hif-1-α negative (figure 11D) show that both appeared to have normal morphology (Figure 11B and D). The cuboidal epithelium was of proper thickness and shape while airway and distal epithelium appear normal. There were no apparent phenotypic differences between Hif-1-α positive and negative lungs at E14.5.

We next examined the effect of deleting Hif-1-α in the lung epithelium on neonatal lungs. Matings described in breeding strategy III produced 3 dead and 3 live triple transgene mice and 5 live double transgenic "wildtype" mice (Figure 12E, C and A, respectively). Pictures of whole triple transgenic and wildtype lungs were taken immediately upon removal (Figure 12 E, C and A, respectively). Lungs in Figure 12 A and C are from mice that lived beyond 4 hours. The lung in figure 12 E is from a dead triple transgenic mouse. There were no observable phenotypical differences with either live wildtype or transgenic lungs as observed under light dissecting scope, while the lung from the dead transgenic presented an abnormally large trachea as well as exaggerated vasculature (figure 12A, C and E). All lungs were of normal size and all lobes are present. Figure 12B, D and F are 5-micron sections of non-transgenic and transgenic lungs stained with H&E. Also, the three different lungs are observed under 20X objective light phase microscope. Lungs from figure 12B appear to have a

normal phenotype while the transgenic lungs from 12D and F appear to have an abnormal phenotype. Transgene negative lungs in 12D have large open airspace that are lined with the proper thickness of epithelial cells both proximal and distally. Transgene positive lungs in figure 12D present very few airways and thick masses of cells where open spaces should be found. Some spaces found in figure 12D lungs are filled with red blood cells. This observation may be the result of aspiration of blood while sacrificing the mouse. The lung from figure 12F is absolutely filled with red blood cells wherever there is space to be filled. This is indicative of hemorrhage and not aspiration of blood because the triple transgenic mouse was dead prior to lung dissection.

Discussion

The overall goal of this project was to elucidate the role hypoxia might play during embryonic mouse lung development. More specifically, what role, if any, hypoxia might play during branching morphogenesis of the developing mouse lung. Several key experiments implicate hypoxia as playing a role in embryonic development. First, it has been established that during development, the embryo becomes hypoxic (Semenza, 99). Also, if the regulated half of the HIF-1 transcription factor, Hif-1-α, is knocked out, early embryonic lethality results (Kotch, 99). These results precluded investigation of the role of Hif-1-α on lung development. However, work on Drosophila has shown that the Drosophila trachea, which is a homolog of the lung, relies upon hypoxia to guide its distal most epithelial edges during development (Jarecki, 99).

The first approach to reaching the goals of this thesis was to perform a gene expression profile. This profile targets genes homologous to those involved in Drosophila trachea branching during development. Branchless (FGF) and Breathless (FGF receptor) are homologous to mammalian FGF10 and FGFR2IIIb, respectively (Sutherland, 96; Klambt, 92). In addition to homologous genes, the mouse lung expresses FGF7 that, like FGF10, binds FGFR2IIIb (Rubin, 89; Miki, 91). The developing Drosophila trachea also

utilizes Trachealess, which is a homolog of mammalian Hif-1-α (Isaac, 96). Trachealess also has an additional mammalian homolog, Hif-2-α (Ema, 97). Hif-2-α responds to low oxygen the same way as Hif-1-a does (Ema, 97). All genes mentioned above were analyzed via reverse transcription and real time PCR.

Real time PCR was performed on a series of mouse lungs that spans E10.5 through E18.5, PND1 and adult. All three genes, FGF10, FGF7 and FGFR2IIIb were dynamic in their expression patterns over time. Interestingly, these three genes exhibited peak expression levels at the same time point, E16.5 (Fig. 4A). Hif-1-α expression levels were also dynamic over time as well, and, like the FGF genes, Hif-1-α exhibited peak expression by E16.5. In contrast, Hif-2-α gene expression declined dramatically by E16.5.

The first question that comes to mind regarding the results from the gene expression profile is whether there is an important developmental process that occurs at E16.5 in the mouse lung. The answer is yes. Around E16.5, the lung transitions from activities supporting branching morphogenesis and cell proliferation to cytodifferentiation of ductal epithelial cells (Mendelson, 00). The increase of genes involved in facilitating branching morphogenesis, FGF10 and the FGFR2IIIb, may be

upregulated dramatically by E16.5 in order to complete that process. It could also be hypothesized that all of the genes involved in this study are upregulated dramatically by E16.5 simply because the size of the lung may increase substantially between E15.5 and E16.5. To further support that hypothesis, the FGFR2IIIb expression may increase on E16.5 due to one final round of dichotomous branching. This activity would increase the proportion of lung distal epithelium, which is where the receptor is expressed (Klambt, 92). Such morphogeneic expansion might require that the mesenchyme surrounding the distal epithelium increase its expression of FGF10 and FGF7.

Finally, Hif-1-α mRNA has been reported to exhibit a relatively unchanging expression level in developing mouse tissues, including lung (Zhu, 96; Jain, 98). Therefore, the Hif-1-α expression peak at E16.5, like that of FGF10 and FGF7, could be due to an increase in lung size. Two findings challenge the lung size to gene expression ratio hypothesis. First, all of the genes that increase expression dramatically by E16.5 also down regulate expression dramatically by E17.5 (Fig. 4A and B) when the lung is still expanding. Second, the Hif-1-α homolog, Hif-2-α, decreases its expression dramatically by E16.5 and then upregulates expression by E17.5.

It is easy to hypothesize from these findings that the increasing levels of FGF10, FGFR2IIIb and Hif-1-α expression facilitate the final stage of branching morphogenesis. A natural extension of this hypothesis is that the developing mouse lung is using similar signaling cascades as the Drosophila trachea. Areas of hypoxia increase the expression of FGF10 in the mesenchyme, along with Hif-1-α in both the mesenchyme and epithelium, which supports the expression of the FGFR2IIIb. It would be easy to conclude that hypoxia and Hif-1-α definitely play a role in branching morphogenesis with the developing mouse lung. Before that conclusion is made, the lung culture data and transgenic animal results must be considered.

Completely different conclusions can be made for the FGF7 and Hif-2-αgene expression results. First, as stated earlier, at E16.5 the lung is transitioning to cytodifferentiation (Mendelson, 00). FGF7 has been found to increase differentiation of alveolar type II cells in culture (Sugahara, 96). This finding is backed up by the fact that cytodifferentiation begins by E16.5 in the mouse lung (Mendelson, 00). Interestingly, it is at this point that the most robust expression of FGF7 was seen. Hif-2-α expression is upregulated dramatically by E17.5. Correlating this observation with data from the Hif-2-αknockout mouse, which exhibits immature type II cells,

supports the hypothesis that FGF7 and Hif-2-α increase gene expression around E16.5 and 17.5 in support of epithelial cytodifferentiation.

We performed experiments using explants of embryonic lungs in order to determine what effects that hypoxia had on the genes of interest from this project. Lungs from E11.5 and E13.5 were cultured 3 days under normoxic (21% oxygen) or hypoxic (3% oxygen) conditions. RNA from these lungs was isolated and genes analyzed via real time PCR. At E11.5, the lungs in hypoxia exhibited thicker and a more 3-dimensional mesenchyme when compared to those cultured in normoxia. This result could be because Hif-1-α, and to a greater extent hypoxia in general, is a mesenchymal survival factor (Semenza, 99). Expression of FGF10 and FGFR2IIIb in E11.5 cultures increased expression 80% and 190% in hypoxic lung while a 40% and 140% increases were seen in normoxic lungs, respectively. These levels were compared to gene expression in E11.5 cd0 lungs and somewhat correspond to what might be seen in *in vivo* lungs 2 to 3 days later in development. These results support the hypothesis that hypoxia increases the expression of genes responsible for branching morphogenesis. These data could also reflect an increase in distal epithelium and its surrounding mesenchyme in hypoxic versus normoxic lungs due to increased branching morphogenesis. If so, this increase would not be due to a general

increase in lung size. Hif-1-α expression, on the other hand, remained unchanged in hypoxia-cultured lungs while normoxic lungs exhibited a 30% increase. Hif-1-α may be regulated by different mechanisms at this point in lung development. Hif-2-α remained constant for both culture conditions.

E13.5 lungs cultured under normoxic and hypoxic conditions revealed different morphological and gene expression results from E11.5. First, there appeared to be no changes in mesenchyme appearance by cd3. Second, there was a distinctly greater number of epithelial branches in hypoxia-cultured lungs when compare to normoxia-cultured lungs by cd3. The observation may reflect the possibility that the lung, by E13.5, may have all the mesenchyme it will produce. The second result could be because, by cd3, an E13.5 lung could be classified as an E16.5 lung. This hypothesis is supported by the fact that, by E16 in vivo, the lung completes its final round of branching morphogenesis, which occurs in a hypoxic environment and may be driven by hypoxia. This hypothesis is further supported when looking at the expression of FGF10 and Hif-1-α from these lungs. By cd3, FGF10 exhibits a 480% increase in expression versus a 40% increase in normoxic lungs, when compared to cd0 lungs. Furthermore, Hif-1-α exhibits a 90% increase in expression from hypoxic cultured lungs versus a 20% increase in normoxic lungs when compared to cd0. Together, when

compared to the data from E11.5 lungs, these data support a model in which E13.5 lungs cultured for 3 days under hypoxic conditions progress in development to a stage similar to an E16.5 lung. The increase in FGF10 and Hif-1-α expression in E13.5 lungs cultured under hypoxia mimics the increase we saw *in vivo* in our gene expression profile. We conclude, therefore, that tissue cultured under hypoxic conditions may recapitulate in vivo conditions better than tissue cultured under normoxic conditions.

Finally, a mouse with a conditional deletion of Hif-1-α in the lung epithelium was analyzed to gain some insight into the possible role of Hif-1-α in branching morphogenesis. In our initial experiment, the pregnant dam was fed doxycycline (dox) beginning 3 days after conception and then sacrificed on E14.5. As can be seen in Figure **11 A and C**, there appears to be no difference in gross morphology. Unfortunately, the results from the developmental profile were not complete by this time otherwise the fetuses would have been analyzed on E17.5, just after the completion of branching morphogenesis. From these data we could not conclude that Hif-1-α plays a role in branching morphogenesis.

Our next approach was to allow a pregnant dam, fed dox beginning 3 days after conception, to go full term. The birth resulted in 3 dead pups and 9 live. The three dead pups genotyped as triple transgene positive, as did 3

live pups (i.e. Hif-1-α deleted in distal epithelium). The other 6 live births genotyped as double transgenic (Hif-1-α positive). Initial observations of whole lungs from live pups did not reveal any major morphological differences (Fig 12 A and C). The dead pups, however, appeared to have abnormally large trachea (Fig 12E). All lobes, the trachea, and vasculature were present nonetheless (Fig 12 A, C and E). Upon closer observation, the triple transgenic lungs from both live and dead animals appeared to have cyst like structures, while the double transgenic lungs were free from such structures. Also, when section histochemistry was performed, differences between the two lungs were found. The double transgenic lungs appeared to have normal and numerous airways (Fig. 12B). The transgene positive lungs from the live births, however, had reduced numbers of airways as well as thicker cell mass between the airways (Fig. 12 D). The three triple transgenic animals that didn't die may reflect a lesser extent of Cre-mediated recombination, which will be analyzed by section *in situ* hybridization in the future. A second possibility is that the Hif-1-α got floxed, but for unknown reasons had a lesser effect on morphogenesis. The morphology seen in these mice look identical to that seen in the Hif-2-α knockouts (Campernolle, 02). Lungs from dead triple transgenic animals have a significant morphological change, i.e. alveolar hemorrhage, which explains why they die (Fig 12 F).

Why did they have alveolar hemorrhage? One good hypothesis is that the vasculature didn't develop properly. This makes a lot of sense when you take into account the fact that one of the first genes known to be regulated by hypoxia and Hif-1-α is VEGF (Shweiki, 92; Ladoux, 93; Ikeada, 95; Kotch, 99). No diagnostic analyses of any of the lungs have been performed, so conclusions can only be drawn about the morphology.

Overall, it is important to note that hypoxia and Hif-1-α must be playing an important role in mouse lung development. First, its expression levels have been found to be dynamic over time (Fig 4 B). In order to back up this result, we plan to perform whole mount *insitu* hybridization (ISH) of Hif-1-α on E10.5 through 14.5 lungs, as well as on E11.5 and 13.5 lungs cultured under hypoxic and normoxic conditions. The probe has been synthesized and the tissue is now available. This approach could reveal changes in spatial and temporal localization in a physiologically dictated fashion. We will also use whole mount ISH to examine the spatial localization of FGF10, FGF7, and FGFR2IIIb in E11.5 and E13.5 lungs cultured under hypoxic and normoxic conditions.

Second, gene expression appears to respond differently in E13.5 hypoxic cultured lungs when compared to not only normoxic lungs, but also E11.5 cultured lungs. For example, it was found that Hif-1-α gene

expression increased in E13.5 hypoxi-cultured lungs while it remained constant at E11.5 lungs cultured under hypoxic conditions. Does the E13.5 lung control Hif-1-α mRNA expression differently than in E11.5 lungs?

Third, does the culture of E13 lungs for 3 days under hypoxic conditions better mimic normal development *in vivo* than when normoxic culture conditions are used? Electron microscopy can be performed and the presence or absence of mature type II cells can be looked for. Also, SP-A, SP-B, SP-C and CC10 gene expression can be analyzed in these lungs via real time PCR.

Finally, we will analyze the triple transgenic mice beyond morphology. If the floxed Hif-1-α phenotype is similar to the Hif-2-α knockout mouse, then electron microscopy needs to be performed in order to assess the condition of the type II cells. An important possible approach would be to use cDNA microarray analysis to assess global changes in gene expression in epithelial cells in which Hif-1-α has been inactivated versus controls. This could reveal changes in genes involved in branching morphogenesis, vascular development, and epithelial differentiation.

Figure 1. Schematic representation of the molecular response to low or normal oxygen tension. Extracellular oxygen tension is first sensed at the plasma membrane. Upon determining if the oxygen tension is normal/normoxic (**Fig. 1a**) or low/hypoxic (**Fig. 1b**), the signal will be transduced to the nucleus where the overall effect will be determined at the transcriptional level.

Figure 1

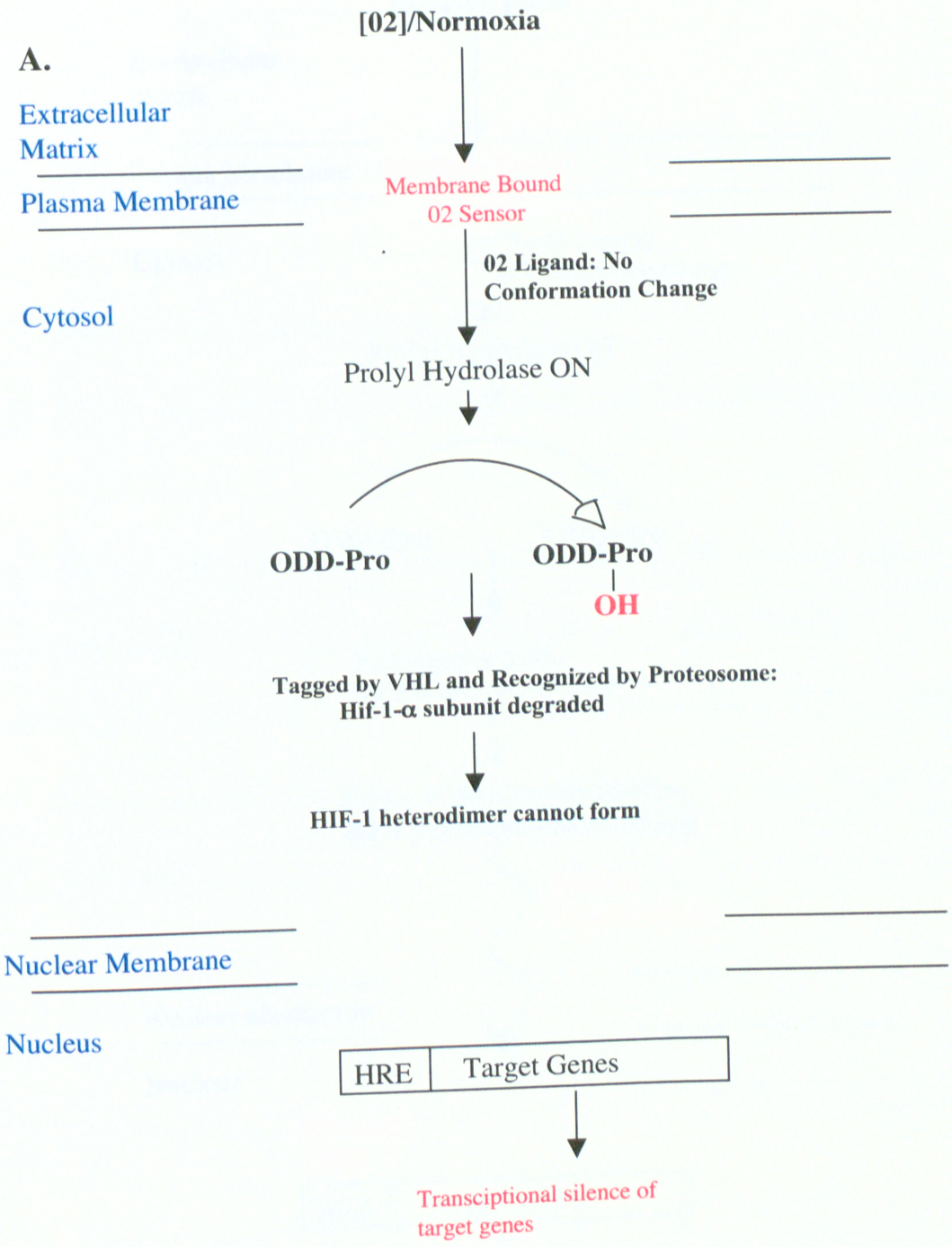
[02]/Normoxia
A.
Extracellular Matrix
Plasma Membrane
Membrane Bound 02 Sensor
02 Ligand: No Conformation Change
Cytosol
Prolyl Hydrolase ON
ODD-Pro
ODD-Pro
OH
Tagged by VHL and Recognized by Proteosome: Hif-1-α subunit degraded
HIF-1 heterodimer cannot form
Nuclear Membrane
Nucleus
HRE
Target Genes
Transciptional silence of target genes

Figure 1

B.

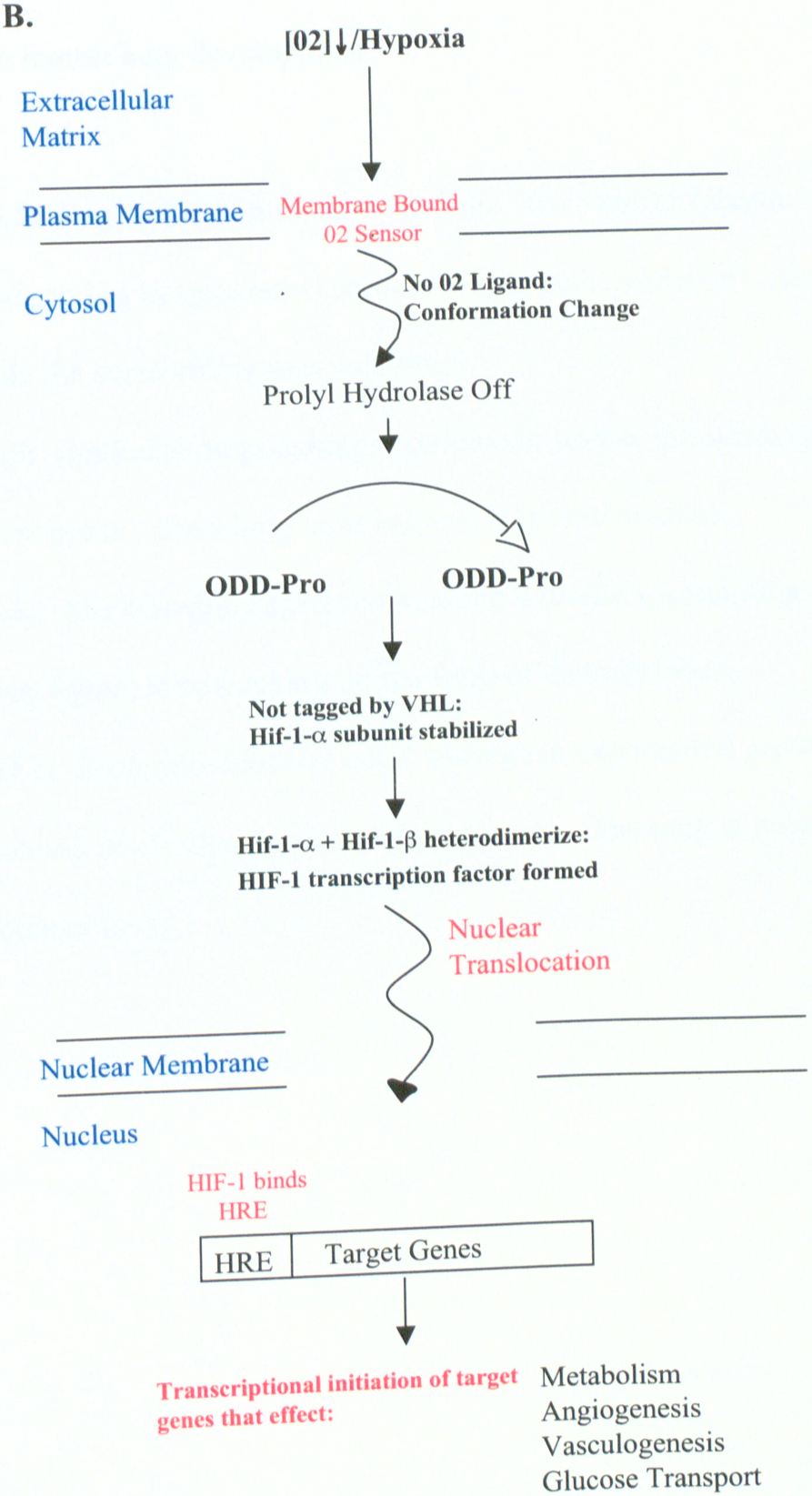
[02]↓/Hypoxia
Extracellular Matrix
Plasma Membrane
Membrane Bound 02 Sensor
Cytosol
No 02 Ligand: Conformation Change
Prolyl Hydrolase Off
ODD-Pro
ODD-Pro
Not tagged by VHL: Hif-1-α subunit stabilized
Hif-1-α + Hif-1-β heterodimerize: HIF-1 transcription factor formed
Nuclear Translocation
Nuclear Membrane
Nucleus
HIF-1 binds HRE
HRE
Target Genes
Transcriptional initiation of target genes that effect:
Metabolism
Angiogenesis
Vasculogenesis
Glucose Transport

Figure 2. Whole lung explants showing the major morphological changes occurring in mouse lung development.

A. **E10.5:** Beginning of lung development. The ventral foregut endoderm has evaginated to form two lung buds, which are starting to invade the surrounding mesenchyme.

B. **E12.5:** Epithelial outpouchings continue to invade the surrounding mesenchyme. Branching morphogenesis is now evident.

C. **E14.5:** The branching epithelium, along with the surrounding mesenchyme, is now taking on the form of distinct lobes.

D. **PND 1:** Each individual lobe has undergone exponential growth and branching while alveolarization is beginning. The lung is now in its functional form.

Figure 2

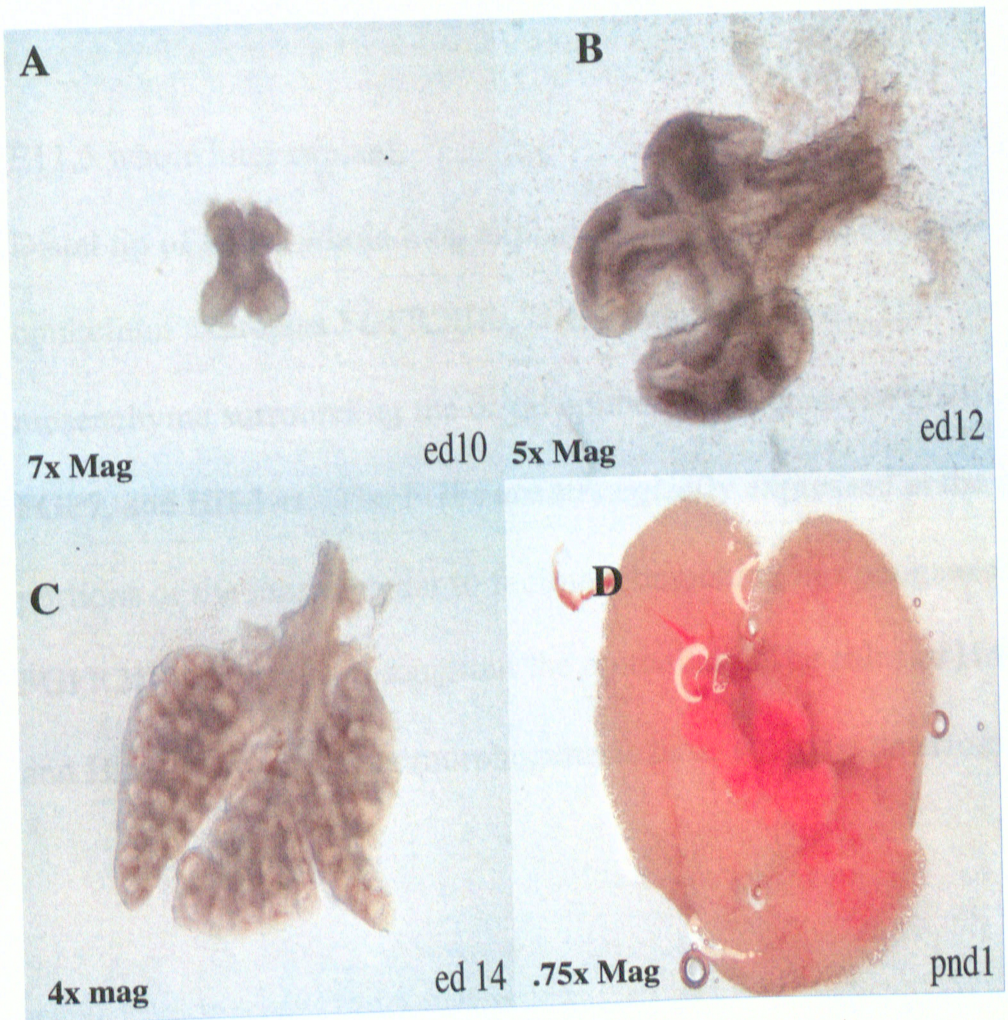

Figure 3: Visual representation of E11.5 lung and the regions in which genes responsible for branching morphogenesis and the hypoxic response genes are located spatially.

a. E11.5 whole lung explant.

b. Distal tip of E11.5 whole lung explant magnified 2X. The distal epithelium expresses FGFR2IIIb, Hif-1-α, and Hif-2-α. The mesenchyme surrounding the distal epithelium expresses FGF10, FGF7, and Hif-1-α. The FGFs are strategically expressed at the distal portions of the lung in order to facilitate branching morphogenesis. FGFR2IIIb is present throughout the epithelium. The roles of Hif-1-α and Hif-2-α in branching morphogenesis have yet to be determined.

Figure 3

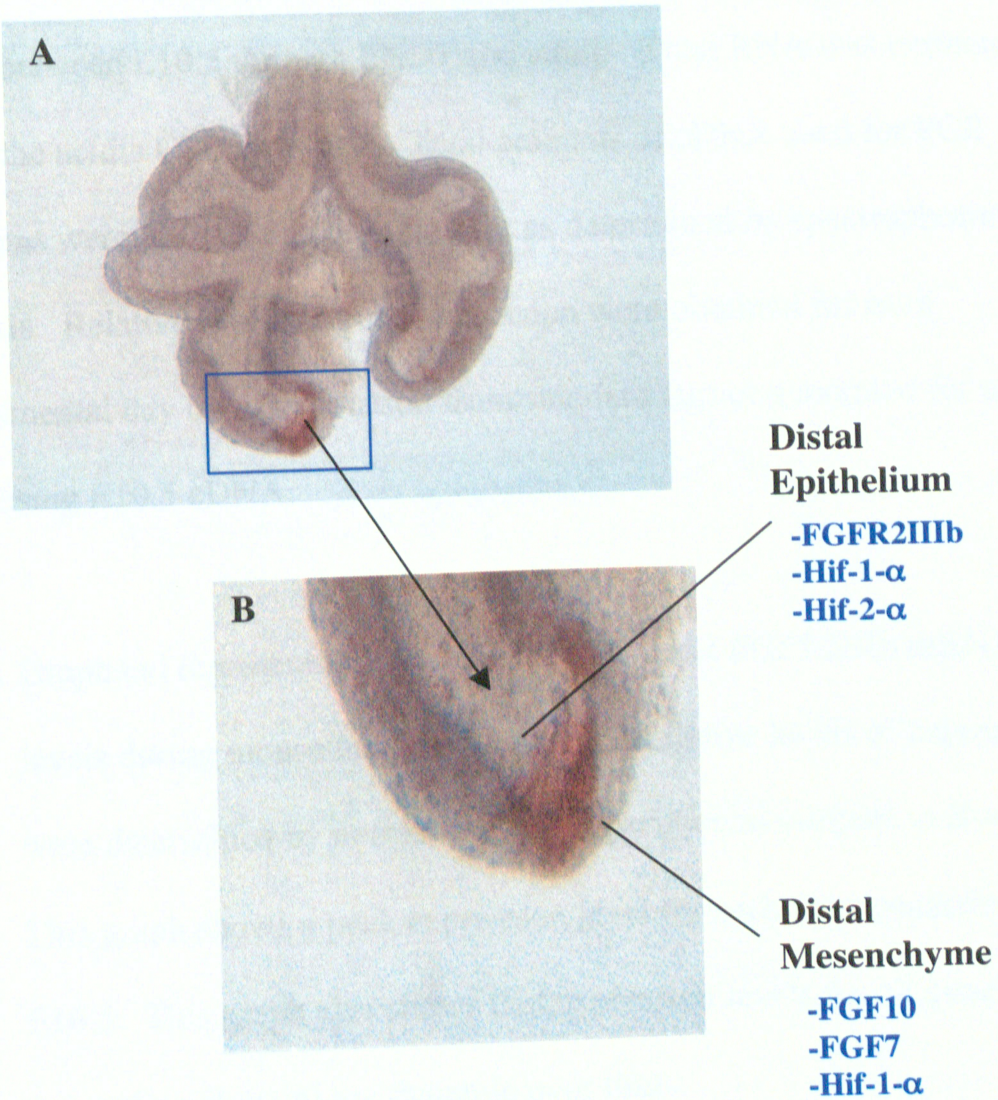
A
B
Distal
Epithelium
-FGFR2IIIb
-Hif-1-α
-Hif-2-α
Distal
Mesenchyme
-FGF10
-FGF7
-Hif-1-α

Figure 4: Developmental profile of gene expression created using real time PCR. Analysis of cDNA synthesized from time staged whole mouse lungs between E10.5 through PND1 and adult. Total RNA was extracted using the acidic GITC protocol. Total amounts of cDNA used for PCR reactions were the same for all samples, as determined by spectrophotomeric analysis. Relative levels of gene expression were obtained for each experimental day by extrapolation from standard curves generated for each gene using E10.5 cDNA.

A. Graphical representation of FGF10, FGF7 and FGFR2IIIb mRNA levels during mouse lung development. Relative levels of expression were determined by normalizing all experimental samples to B-actin. This graph shows a peak expression level for each gene occurring by E16.5. This graph also shows that expression levels for all genes (excluding B-actin) are dynamic over time.

B. Graphical representation of genes involved in the molecular response to hypoxia. Hif-1-α and Hif-2-α mRNA levels were determined by normalizing all experimental samples to B-actin. This graph shows a peak expression level for Hif-1-α occurring by E16.5 while its homolog, Hif-2-α, is at its lowest by this day.

Figure 4

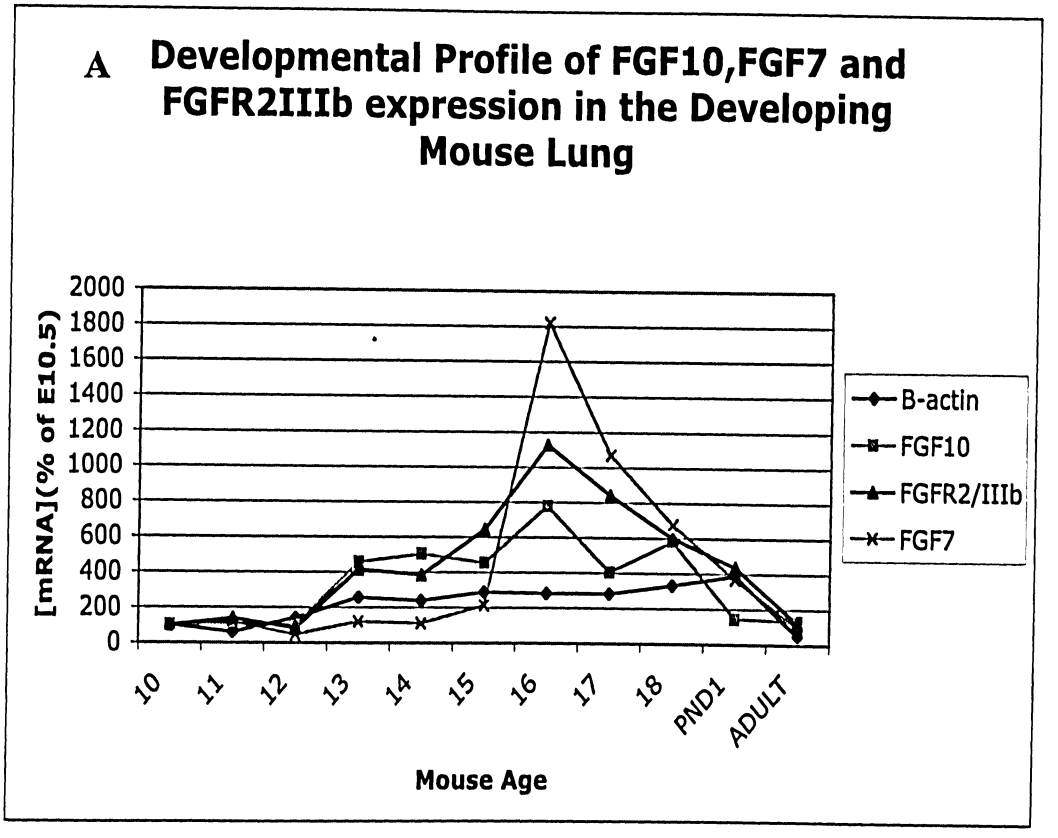
A
Developmental Profile of FGF10,FGF7 and FGFR2IIIb expression in the Developing Mouse Lung
[mRNA](% of E10.5)
2000
1800
1600
1400
1200
1000
800
600
400
200
0
10
11
12
13
14
15
16
17
18
PND1
ADULT
Mouse Age
B-actin
FGF10
FGFR2/IIIb
FGF7

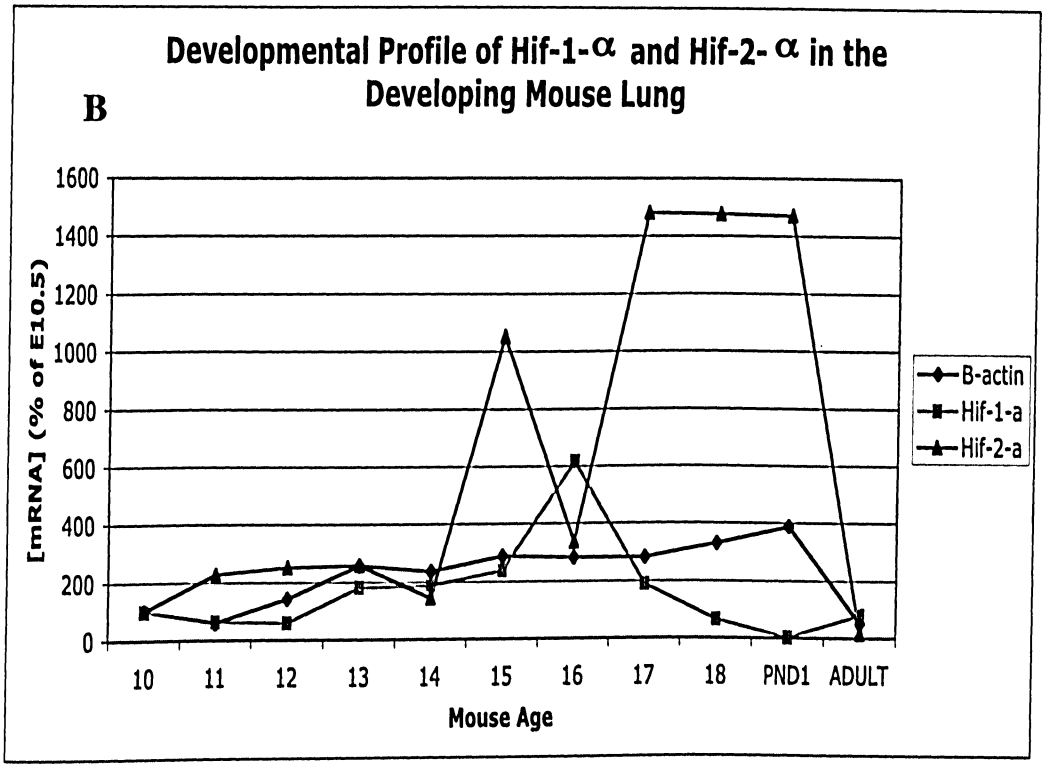
Developmental Profile of Hif-1-α and Hif-2-α in the Developing Mouse Lung
B
[mRNA] (% of E10.5)
1600
1400
1200
1000
800
600
400
200
0
10
11
12
13
14
15
16
17
18
PND1
ADULT
Mouse Age
B-actin
Hif-1-a
Hif-2-a

Figure 5: Whole embryonic lung explants cultured in normoxic (21% oxygen) or hypoxic (3% oxygen) conditions. Lungs were removed from time-staged embryos at E11.5 and immediately placed into GITC for culture day (cd) 0 controls. Lungs for culture were placed onto semisolid agarose medium and covered with sufficient DMEM/F12 plus 5% FBS to create an air-liquid interface. Lungs destined for culture were separated into 2 groups depending upon oxygen levels.

A. Pictures of whole E11.5 lung explants on culture day (cd) 0, 1, 2, and 3 maintained under normoxic (N) conditions. Exactly 24 hours passed prior to each photograph taken. Cultured lungs were analyzed via basic morphology and viewed using a dissecting scope.

B. Same as A but lungs were cultured under hypoxic (H) conditions.

Note the differences in appearance of the mesenchyme when comparing cd3 N cultured lungs to cd3 H cultured lungs. The hypoxic lung mesenchyme has a 3-dimensional appearance while the normoxic lungs flatten out on the agarose.

Figure 5

E11.5 Lung Explant Culture Experiment

A.

21% Oxygen(Normoxic)

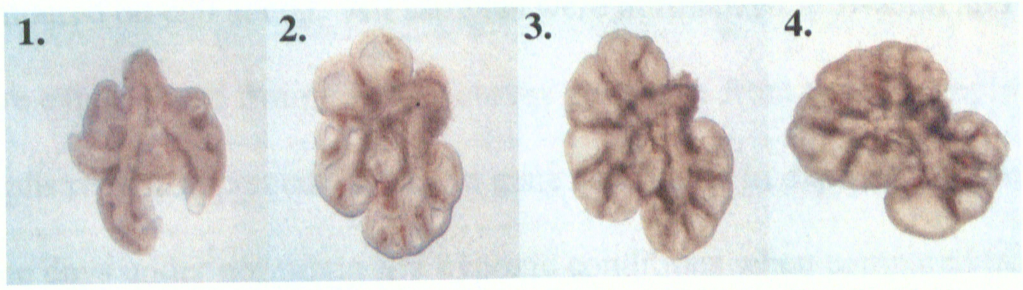

E11.5 cd0 N E11.5 cd1 N E11.5 cd2 N E11.5 cd3 N

B.

3% Oxygen(Hypoxic)

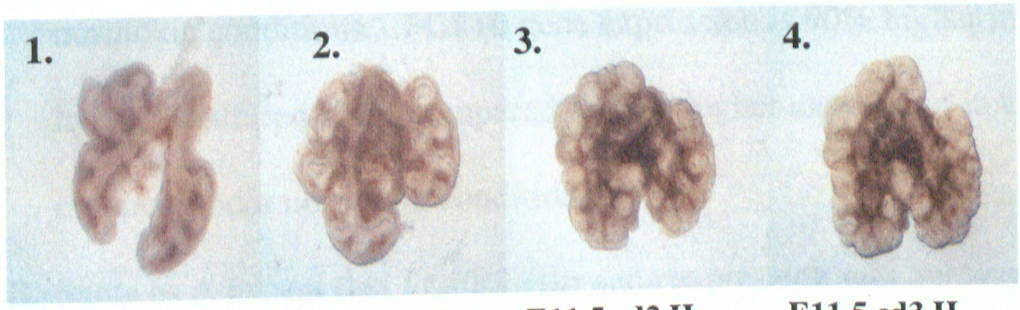

E11.5 cd0 H E11.5 cd1 H E11.5 cd2 H E11.5 cd3 H

Figure 6: Lungs from Figure 5 were subjected to GITC extraction of total RNA and reverse transcription. The resulting cDNA was analyzed by real time PCR analysis, then hypoxic and normoxic experimental samples were compared on cd0 at cd3. All samples were normalized to B-actin and values were extrapolated from standard curves generated from time 0 samples. The graphs represent percent change in gene expression in explants cultured three days under normoxic and hypoxic conditions when compared to cd0 explants.

A. Effect oxygen tension has on FGF10 from cDNA synthesized from ED11.5 whole lung extracts cultured for 3 days under hypoxic and normoxic conditions. FGF10 gene expression is 90% higher in hypoxic cultured lungs compared to 40% higher expression in those cultured under normoxic conditions.

B. Same as A except that FGFR2/IIIb gene expression was analyzed. FGFR2IIIb gene expression is 190% higher in hypoxic cultured lungs compared to 140% higher expression in those cultured under normoxic conditions.

C. Same as A except that HIF-1-α gene expression was analyzed. Hif-1-α gene expression did not change in cd3 hypoxic explants, while expression in normoxic explants increased 30%.

D. Same as A except that Hif-2-α gene expression was analyzed. Hif-2-α gene expression decreased by 10% in hypoxic explants, while expression in normoxic explants increased 10%.

Figure 6

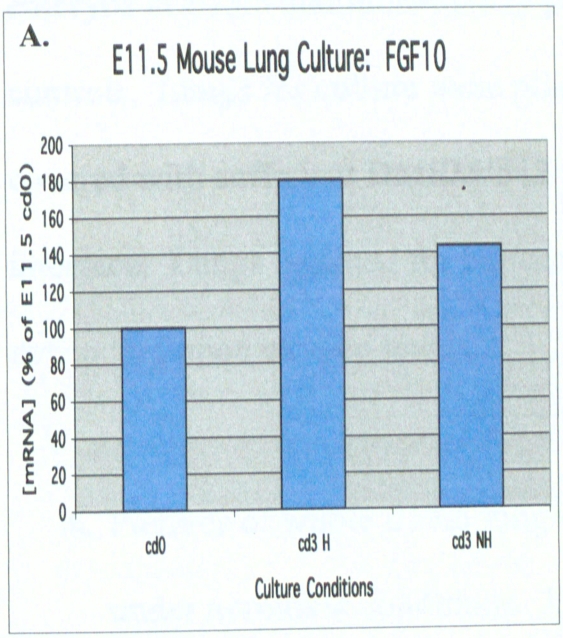
A.
E11.5 Mouse Lung Culture: FGF10
[mRNA] (% of E11.5 cd0)
0
20
40
60
80
100
120
140
160
180
200
cd0
cd3 H
cd3 NH
Culture Conditions

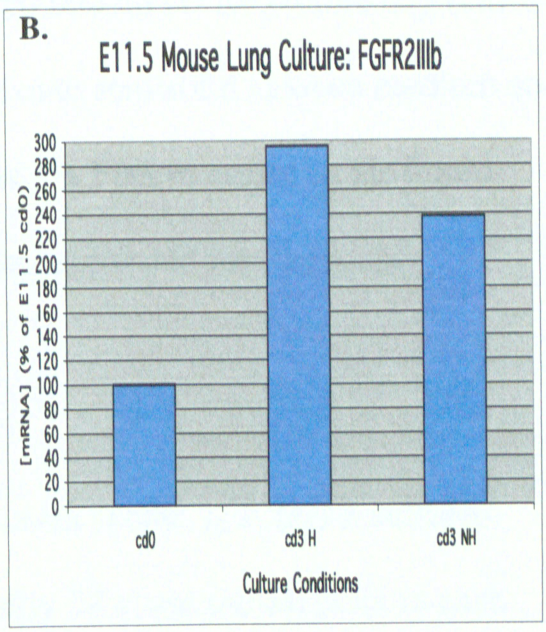
B.
E11.5 Mouse Lung Culture: FGFR2IIIb
[mRNA] (% of E11.5 cd0)
0
20
40
60
80
100
120
140
160
180
200
220
240
260
280
300
cd0
cd3 H
cd3 NH
Culture Conditions

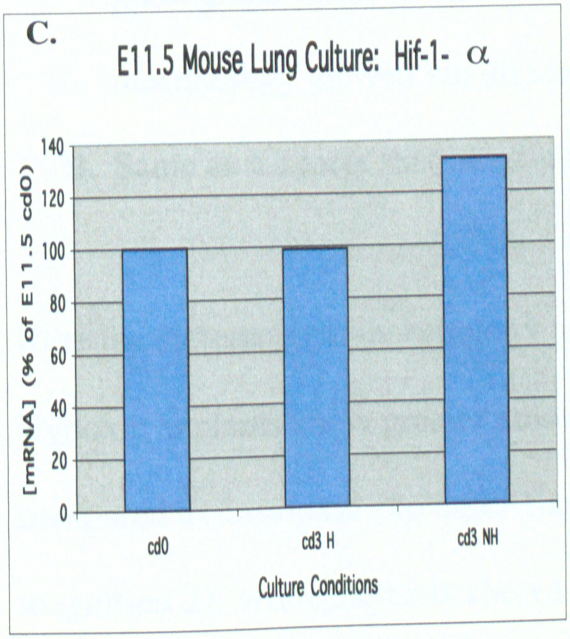
C.
E11.5 Mouse Lung Culture: Hif-1- α
[mRNA] (% of E11.5 cd0)
0
20
40
60
80
100
120
140
cd0
cd3 H
cd3 NH
Culture Conditions

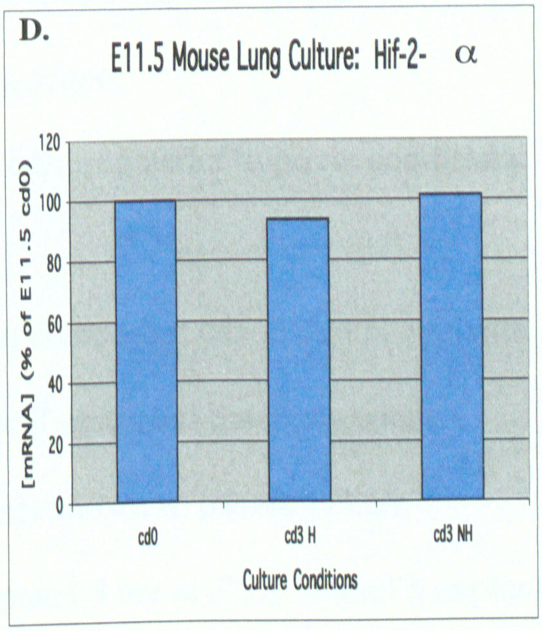
D.
E11.5 Mouse Lung Culture: Hif-2- α
[mRNA] (% of E11.5 cd0)
0
20
40
60
80
100
120
cd0
cd3 H
cd3 NH
Culture Conditions

Figure 7: Whole lung explants cultured under normoxic (21% oxygen) or hypoxic (3% oxygen) conditions. Lungs were removed from time-staged embryos at E13.5 and immediately placed into GITC for culture day (cd) 0 controls. Lungs for culture were placed onto semisolid agarose medium and covered with sufficient DMEM/F12 plus 5% FBS to create an air-liquid interface. Lungs destined for culture were separated into 2 groups depending upon oxygen levels.

A. Pictures of whole E13.5 lung explants at cd0, 1, 2, and 3 cultured under normoxic conditions. Exactly 24 hours passed prior to each photograph taken. Cultured lungs were analyzed via basic morphology viewed via dissecting scope.

B. Same as a except that lungs were cultured under hypoxic conditions.

Note the difference in morphology when comparing cd3 H and N explants. Hypoxic explants show greater amounts of epithelial branches when compared to normoxic explants. Explants shown in panels 1-3 are magnified 2X while explants shown in panel 3 are at .75X. Panel 3 explants are magnified .75X in order to fit entire lung into picture.

Figure 7

E13.5 Lung Explant Culture Experiment

A. 21% Oxygen(Normoxic)

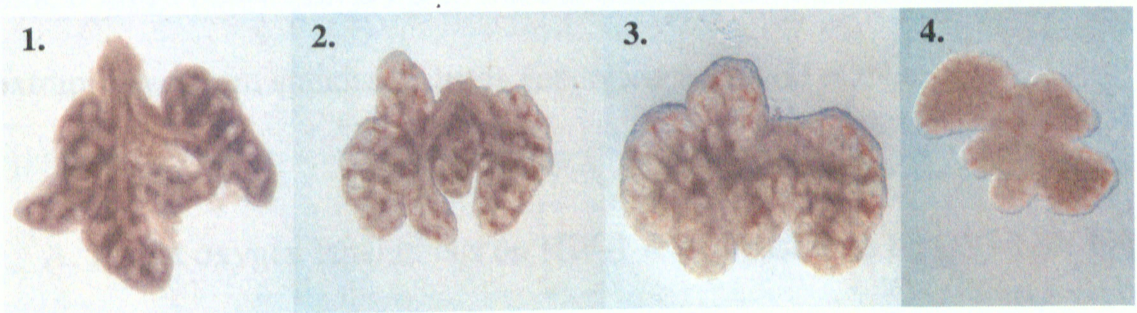

E 13.5 cd0 N E 13.5 cd1 N E 13.5 cd2 N E 13.5 cd3 N

B. 3% Oxygen(Hypoxic)

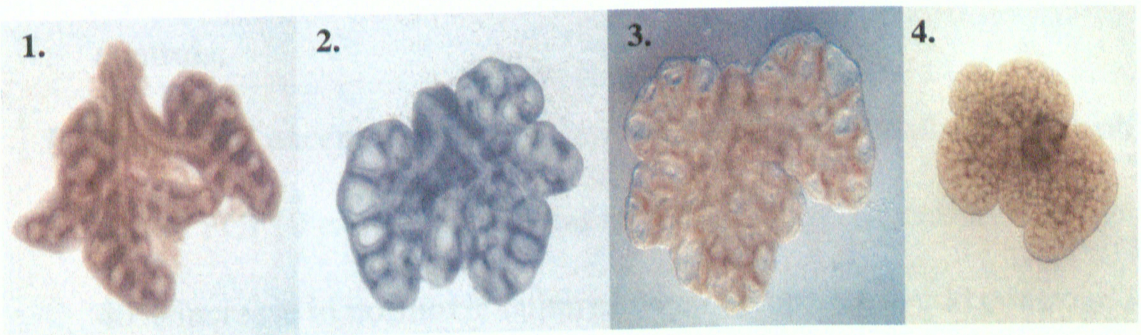

E 13.5 cd0 H E 13.5 cd1 H E 13.5 cd2 H E 13.5 cd3 H

Figure 8: RNA was extracted from lungs cultured as in figure 7 and subjected to reverse transcription. The resulting cDNA was analyzed by real time PCR analysis for Hif-1-α and FGF10. Samples cultured for 3 days under hypoxic (cd3H) and normoxic (cd3N) conditions were compared to time 0 lungs (cd0). All samples were normalized to B-actin and values were extrapolated from standard curves generated from cd0 cDNA.

A. Effect oxygen tension has on HIF-1-α expression in E11.5 whole lung explants cultured for 3 days under hypoxic and normoxic conditions. Experimental samples were compared to the cd0 standard curve data. Graph shows Hif-1-α expression increases 90% in hypoxic cultures and a 20% increase in normoxic cultures when compared to cd0 controls.

B. Same as A except that FGF10 gene expression was analyzed. Graph shows FGF10 expression increases 480% in hypoxic cultures and a 40% increase in normoxic cultures when compared to cd0 controls.

Figure 8

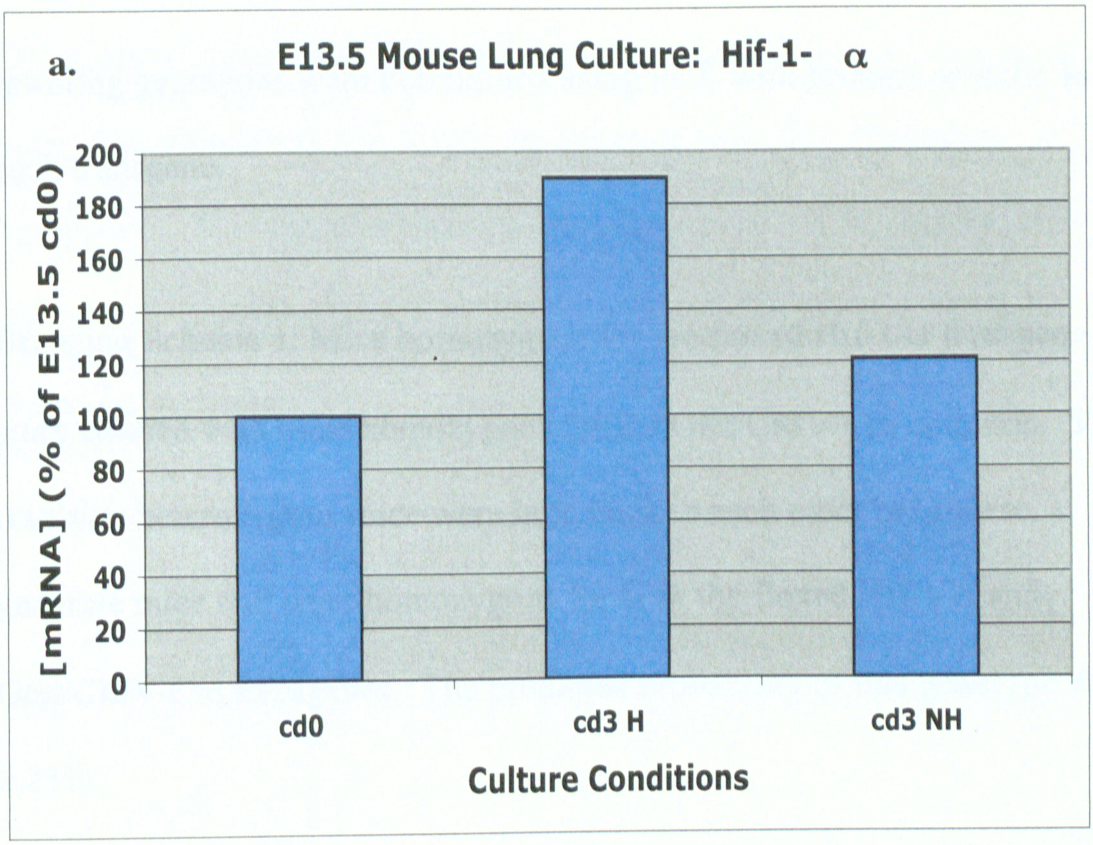
a.
E13.5 Mouse Lung Culture: Hif-1- α
[mRNA] (% of E13.5 cd0)
200
180
160
140
120
100
80
60
40
20
0
cd0
cd3 H
cd3 NH
Culture Conditions

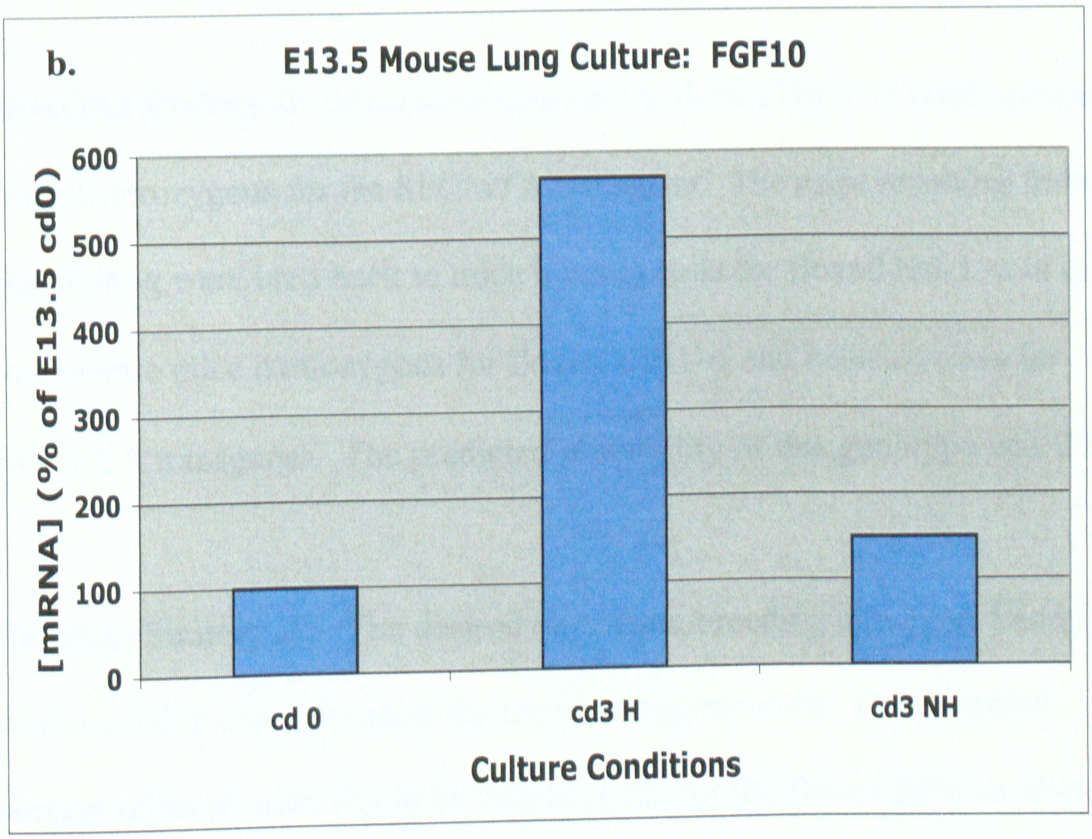
b.
E13.5 Mouse Lung Culture: FGF10
[mRNA] (% of E13.5 cd0)
600
500
400
300
200
100
0
cd 0
cd3 H
cd3 NH
Culture Conditions

Figure 9: Breeding scheme used to create triple transgenic mice. All resulting genotypes were determined using PCR with primers specific to each transgene.

Breeding Scheme 1: Mice homozygous for the floxed Hif-1-α transgene were crossed with mice homozygous for the Otet/CMV/Cre chimeric. The resulting heterozygous mice were bred back to each other in order to generate mice that were homozygous for both the floxed Hif-1-α and Otet/CMV/Cre transgenes. The predicted probability of this genotype was 6.25%.

Breeding Strategy II: Mice homozygous for floxed Hif-1-α were crossed to mice heterozygous for the SPC/rtTA transgene. The mice resulting from this mating were bred back to mice homozygous for floxed Hif-1-α in order to generate mice homozygous for floxed Hif-1-α and heterozygous for SPC/rtTA transgenes. The predicted probability of this genotype was 25%.

Breeding Strategy III: The desired mice from breeding strategies I and II were mated in order to create the triple transgenic mice. One hundred percent of these mice would be homozygous for the floxed Hif-1-α allele

and heterozygous for Otet/CMV/Cre. The predicted occurrence of the SPC/rtTA transgene was 50%. Females from breeding plan I or II were used. The females used were put on doxicycline food 3 days after conception. The resulting litter was genotyped via PCR for each of the 3 transgenes. Those with the SPC/rtTA transgene were considered to be triple transgenic.

Figure 9

Breeding Strategy #1: Generation of Cre/Cre, Flox Hif/Flox Hif Mice

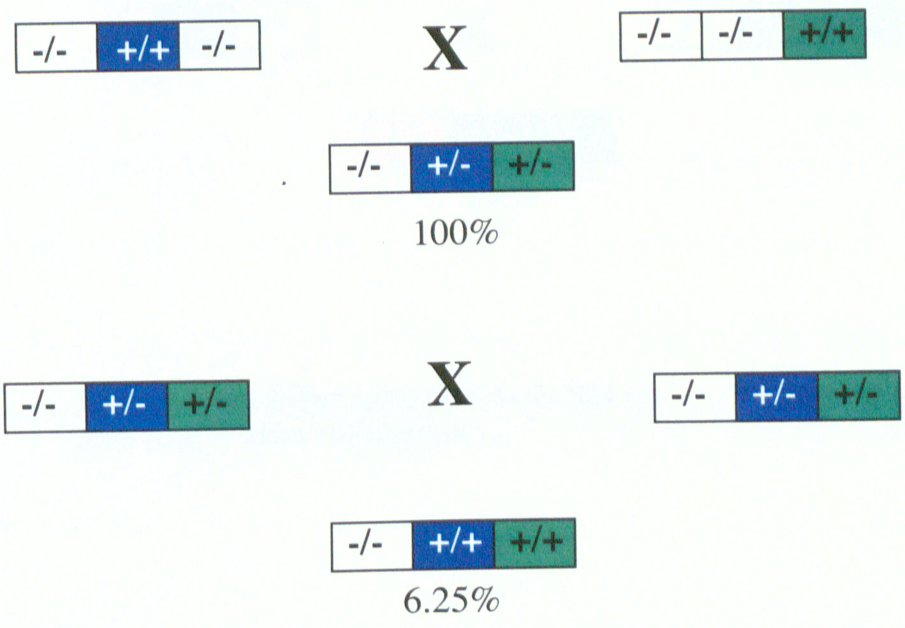

Breeding Strategy #2: Generation of SPCrtTA +/-, Flox Hif/Flox Hif Mice

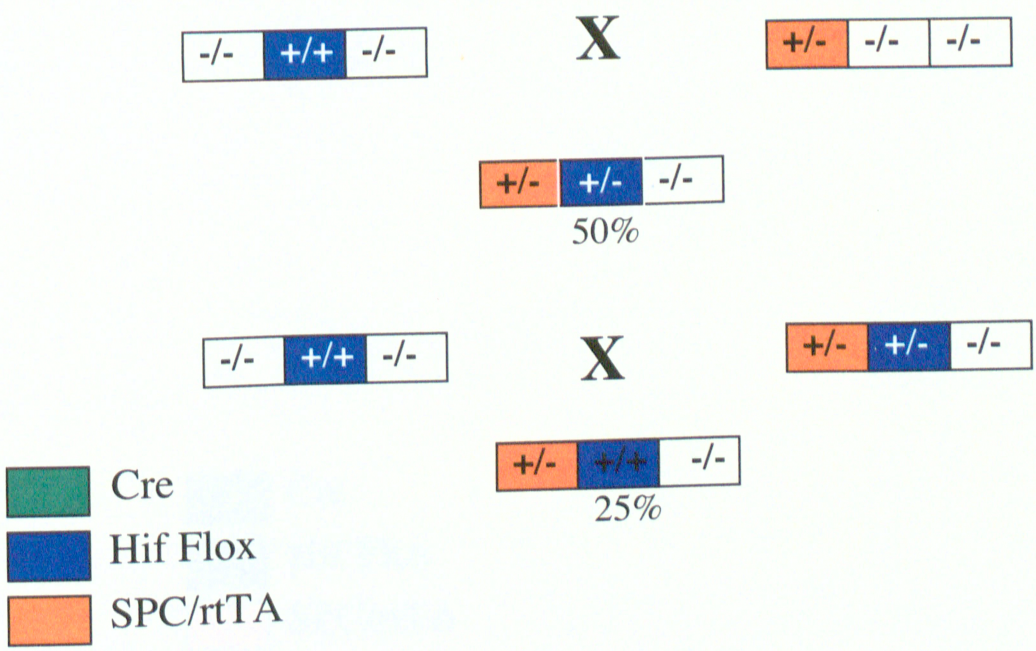

Breeding Strategy #3: Combine final product from #1 and #2

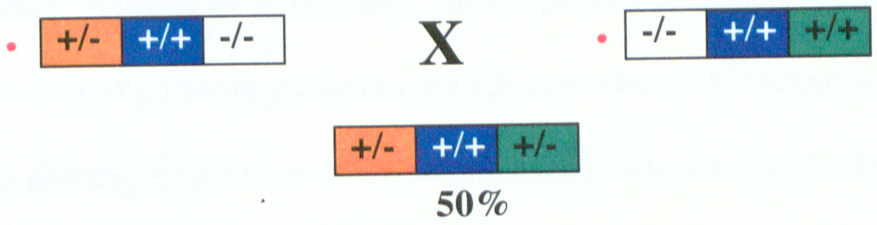

- **Female from either genotype to be put on Dox 3 days after conception**

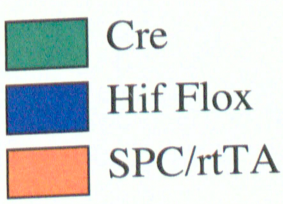

Figure 10: Schematic representation of the Hif-1-α gene is conditionally deleted. Expression of rtTA is driven by the SPC promoter which is active only in the distal epithelium of the lung. In the presence of doxycycline, rtTA binds to Otet regulatory elements, which activates CMV promoter activity, then driving expression of Cre recombinase specifically in the distal lung epithelium. Hif-1-α is deleted only where Cre recombinase is expressed, which is at the distal epithelium. This creates a situation where conditional expression of transgenes can be regulated both spatially and temporally.

Figure 10

1. Distal Epithelial specific Promoter Active, Drives Expression of rtTA

2. Doxicycline is ingested by pregnant dam, circulates system, and binds rtTA where its expression is driven by SPC promoter

2. SPC rtTA binds doxicycline, then locates transactivator present on Cre recombinase transgene, driving Cre recombinase expression

3. Cre Recombinase now interacts with loxP sites that flank Hif-1-α floxed transgene

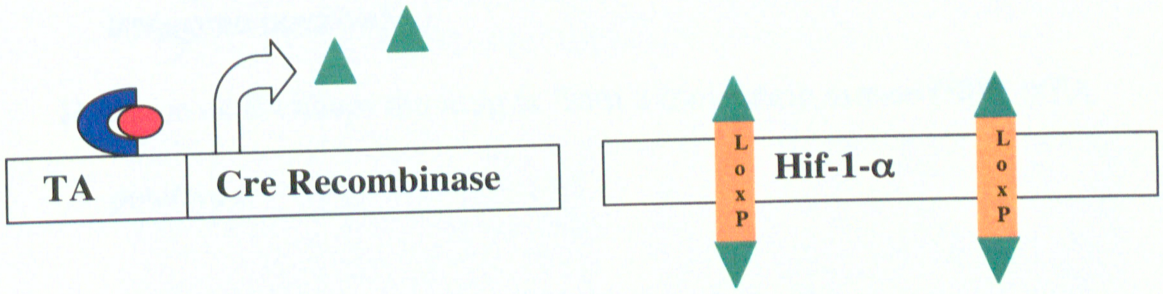

4. Cre recombinase initiates homologous recombination at flanking LoxP sites and Hif-1-α is excised from genome conditionally only where SPC drives rtTA expression

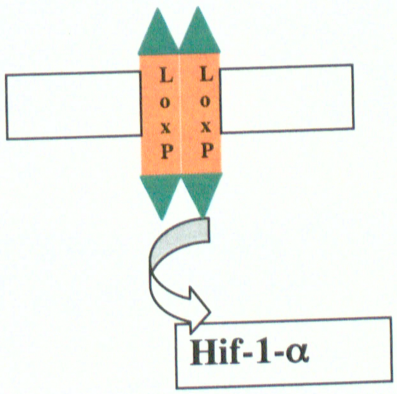

Figure 11: Morphology of lungs from triple transgenic mice on E14.5.

Lungs from transgenic animals were first photographed whole then fixed in paraformaldehyde and processed for paraffin sections 5microns thick.

A. Whole lung dissected from E14.5 wildtype (SPC rtTA negative) mouse observed under dissecting light microscope at 3X.

B. Sectioned and H&E stained lungs from wiltype (SPCrtTa transgene negative) observed using 20X objective on a light microscope.

C. Same as A except the lung is from a transgenic mouse (SPCrtTA transgene positive).

D. Same as B except the lung is from a transgenic mouse (SPC rtTA positive).

Note that both wildtype and transgenic lungs are of equal size and all lobes are present.

Figure 11

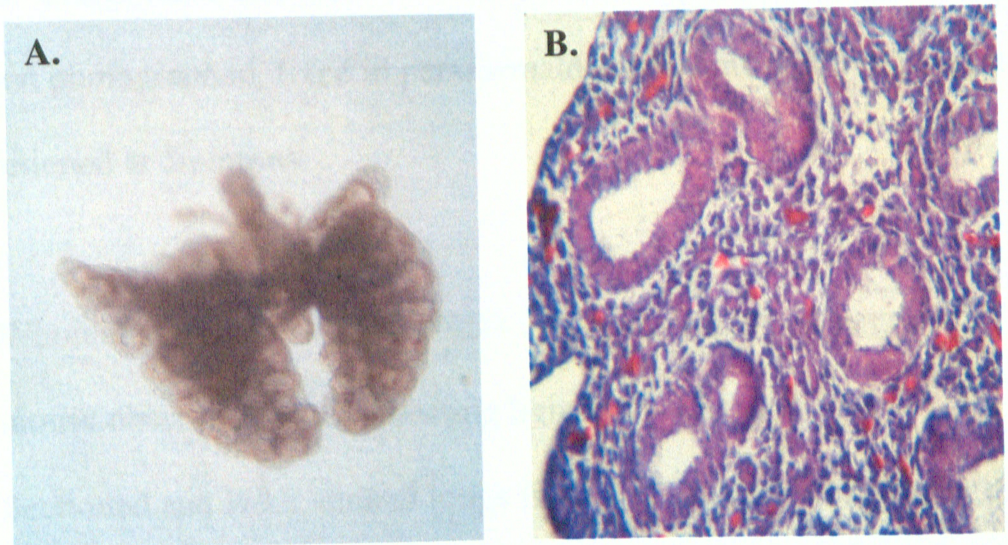

Double Transgenic, intact Hif-1-α:
SPC/rtTA-/-; Floxed Hif-1-α +/+; Cre +/-

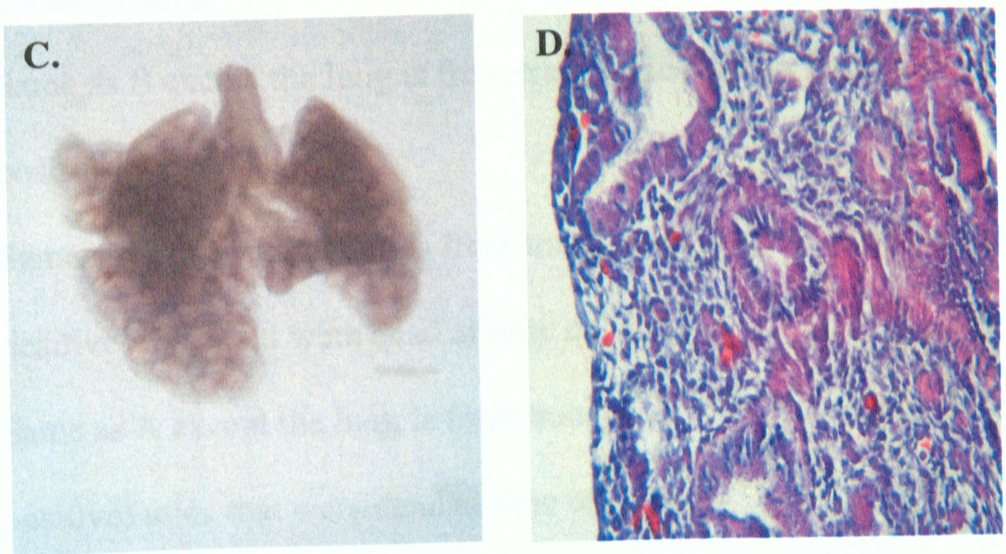

Triple Transgenic, deleted Hif-1-α: SPC/rtTA +/-
; Floxed Hif-1-α +/+; Cre +/+

Figure 12: Morphology of lungs from neonatal triple transgenic animals. Lungs from transgenic animals taken within 4 hours after birth were first photographed, fixed in paraformaldehyde, embedded in paraffin then sectioned at 5microns.

A. Whole lung dissected from PND1 wildtype (SPC/rtTA negative) mouse observed under dissecting light microscope at .75X.

B. Sectioned and H&E stained lungs from wiltype (SPC/rtTa transgene negative) observed using 20X objective on a light microscope.

C. Same as A except the lung is from transgenic (SPC/rtTA transgene positive) mice.

D. Same as B except the lung is from transgenic (SPC/rtTA transgene positive) mice.

E. Same as A except the lung is from transgenic (SPC/rtTA transgene positive) mice that were dead at time of birth.

F. Same as A except the lung is from transgenic (SPC/rtTA transgene positive) mice that were dead at time of birth.

Note that the three lungs in this figure have all lobes present. The lung in panels A and B have normal airspaces and look expanded. The lung in panels C and D appear compacted with less airspaces than in A and B. The

Figure 12

Wildtype: SPC rtTA-/-; Floxed Hif-1-α +/+; Cre +/-, live birth

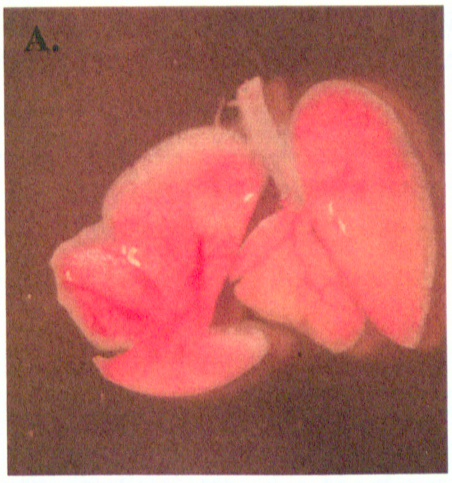

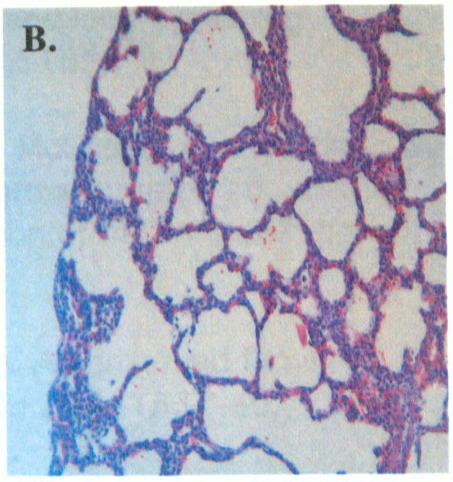

Transgenic: SPC rtTA +/-; Floxed Hif-1-α +/+; Cre +/-, live birth

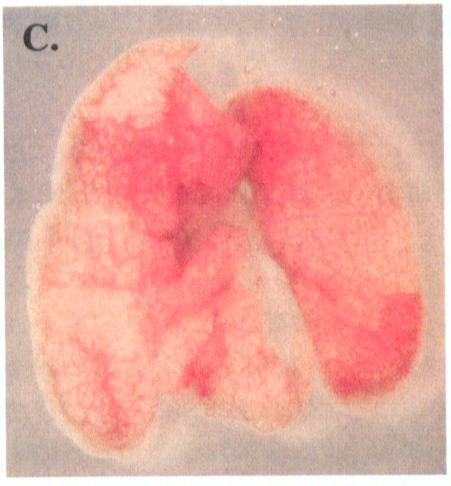

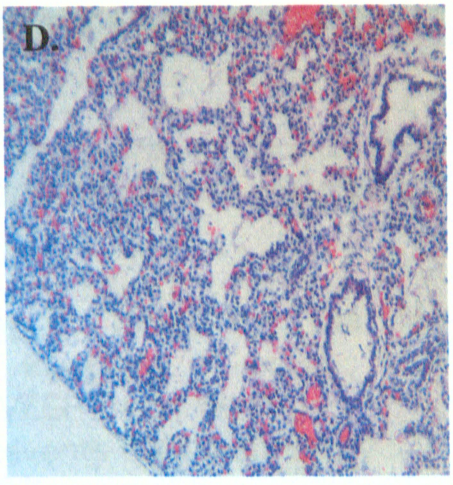

Transgenic: SPC rtTA +/-; Floxed Hif-1-α +/+; Cre +/-, dead at birth

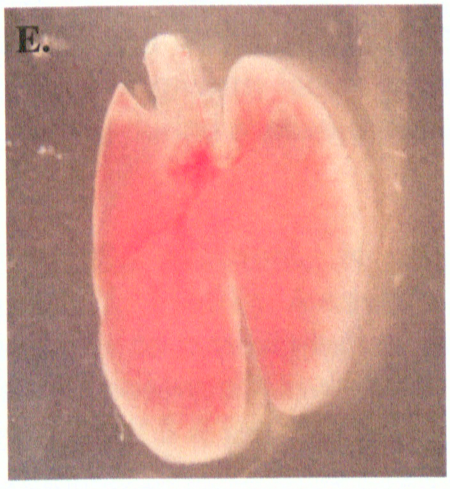

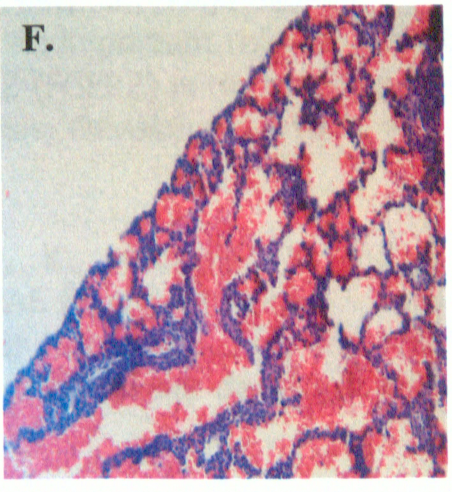

REFERENCES

Arman, E., Haffner-Krausz, R., Gorivodsky, M. and Lonai, P. (1999). Fgfr2 is required for limb outgrowth and lung-branching morphogenesis. *Proc Natl Acad Sci U S A* **96**, 11895-9.

Beer, H. D., Florence, C., Dammeier, J., McGuire, L., Werner, S. and Duan, D. R. (1997). Mouse fibroblast growth factor 10: cDNA cloning, protein characterization, and regulation of mRNA expression. *Oncogene* **15**, 2211-8.

Bruick, R. K. and McKnight, S. L. (2001). A conserved family of prolyl-4-hydroxylases that modify HIF. *Science* **294**, 1337-40.

Celli, G., LaRochelle, W. J., Mackem, S., Sharp, R. and Merlino, G. (1998). Soluble dominant-negative receptor uncovers essential roles for fibroblast growth factors in multi-organ induction and patterning. *Embo J* **17**, 1642-55.

Chomczynski, P. and Sacchi, N. (1987). Single-step method of RNA isolation by acid guanidinium thiocyanate-phenol-chloroform extraction. *Anal Biochem* **162**, 156-9.

Compernolle, V., Brusselmans, K., Acker, T., Hoet, P., Tjwa, M., Beck, H., Plaisance, S., Dor, Y., Keshet, E., Lupu, F. et al. (2002). Loss of HIF-2alpha and inhibition of VEGF impair fetal lung maturation, whereas treatment with VEGF prevents fatal respiratory distress in premature mice. *Nat Med* **8**, 702-10.

De Moerlooze, L., Spencer-Dene, B., Revest, J., Hajihosseini, M., Rosewell, I. and Dickson, C. (2000). An important role for the IIIb isoform of fibroblast growth factor receptor 2 (FGFR2) in mesenchymal-epithelial signalling during mouse organogenesis. *Development* **127**, 483-92.

Ema, M., Taya, S., Yokotani, N., Sogawa, K., Matsuda, Y. and Fujii-Kuriyama, Y. (1997). A novel bHLH-PAS factor with close sequence similarity to hypoxia-inducible factor 1alpha regulates the VEGF expression and is potentially involved in lung and vascular development. *Proc Natl Acad Sci U S A* **94**, 4273-8.

Hilfer, S. R. (1996). Morphogenesis of the lung: control of embryonic and fetal branching. *Annu Rev Physiol* **58**, 93-113.

Ikeda, E., Achen, M. G., Breier, G. and Risau, W. (1995). Hypoxia-induced transcriptional activation and increased mRNA stability of vascular endothelial growth factor in C6 glioma cells. *J Biol Chem* **270**, 19761-6.

Isaac, D. D. and Andrew, D. J. (1996). Tubulogenesis in Drosophila: a requirement for the trachealess gene product. *Genes Dev* **10**, 103-17.

Ivan, M., Kondo, K., Yang, H., Kim, W., Valiando, J., Ohh, M., Salic, A., Asara, J. M., Lane, W. S. and Kaelin, W. G., Jr. (2001). HIFalpha targeted for VHL-mediated destruction by proline hydroxylation: implications for O2 sensing. *Science* **292**, 464-8.

Jaakkola, P., Mole, D. R., Tian, Y. M., Wilson, M. I., Gielbert, J., Gaskell, S. J., Kriegsheim, A., Hebestreit, H. F., Mukherji, M., Schofield, C. J. et al. (2001). Targeting of HIF-alpha to the von Hippel-Lindau ubiquitylation complex by O2-regulated prolyl hydroxylation. *Science* **292**, 468-72.

Jain, S., Maltepe, E., Lu, M. M., Simon, C. and Bradfield, C. A. (1998). Expression of ARNT, ARNT2, HIF1 alpha, HIF2 alpha and Ah receptor mRNAs in the developing mouse. *Mech Dev* **73**, 117-23.

Jarecki, J., Johnson, E. and Krasnow, M. A. (1999). Oxygen regulation of airway branching in Drosophila is mediated by branchless FGF. *Cell* **99**, 211-20.

Klambt, C., Glazer, L. and Shilo, B. Z. (1992). breathless, a Drosophila FGF receptor homolog, is essential for migration of tracheal and specific midline glial cells. *Genes Dev* **6**, 1668-78.

Kotch, L. E., Iyer, N. V., Laughner, E. and Semenza, G. L. (1999). Defective vascularization of HIF-1alpha-null embryos is not associated with VEGF deficiency but with mesenchymal cell death. *Dev Biol* **209**, 254-67.

Ladoux, A. and Frelin, C. (1993). Hypoxia is a strong inducer of vascular endothelial growth factor mRNA expression in the heart. *Biochem Biophys Res Commun* **195**, 1005-10.

Masters, J. R. (1976). Epithelial-mesenchymal interaction during lung development: the effect of mesenchymal mass. *Dev Biol* **51**, 98-108.

Mendelson, C. R. (2000). Role of transcription factors in fetal lung development and surfactant protein gene expression. *Annu Rev Physiol* **62**, 875-915.

Metzger, R. J. and Krasnow, M. A. (1999). Genetic control of branching morphogenesis. *Science* **284**, 1635-9.

Miki, T., Fleming, T. P., Bottaro, D. P., Rubin, J. S., Ron, D. and Aaronson, S. A. (1991). Expression cDNA cloning of the KGF receptor by creation of a transforming autocrine loop. *Science* **251**, 72-5.

Min, H., Danilenko, D. M., Scully, S. A., Bolon, B., Ring, B. D., Tarpley, J. E., DeRose, M. and Simonet, W. S. (1998). Fgf-10 is required for both limb and lung development and exhibits striking functional similarity to Drosophila branchless. *Genes Dev* **12**, 3156-61.

Ohshiro, T., Emori, Y. and Saigo, K. (2002). Ligand-dependent activation of breathless FGF receptor gene in Drosophila developing trachea. *Mech Dev* **114**, 3-11.

Ohshiro, T. and Saigo, K. (1997). Transcriptional regulation of breathless FGF receptor gene by binding of TRACHEALESS/dARNT heterodimers to three central midline elements in Drosophila developing trachea. *Development* **124**, 3975-86.

Ornitz, D. M., Xu, J., Colvin, J. S., McEwen, D. G., MacArthur, C. A., Coulier, F., Gao, G. and Goldfarb, M. (1996). Receptor specificity of the fibroblast growth factor family. *J Biol Chem* **271**, 15292-7.

Park, W. Y., Miranda, B., Lebeche, D., Hashimoto, G. and Cardoso, W. V. (1998). FGF-10 is a chemotactic factor for distal epithelial buds during lung development. *Dev Biol* **201**, 125-34.

Perl, A. K. and Whitsett, J. A. (1999). Molecular mechanisms controlling lung morphogenesis. *Clin Genet* **56**, 14-27.

Peters, K. G., Werner, S., Chen, G. and Williams, L. T. (1992). Two FGF receptor genes are differentially expressed in epithelial and mesenchymal tissues during limb formation and organogenesis in the mouse. *Development* **114**, 233-43.

Powers, C. J., McLeskey, S. W. and Wellstein, A. (2000). Fibroblast growth factors, their receptors and signaling. *Endocr Relat Cancer* **7**, 165-97.

Rubin, J. S., Osada, H., Finch, P. W., Taylor, W. G., Rudikoff, S. and Aaronson, S. A. (1989). Purification and characterization of a newly identified growth factor specific for epithelial cells. *Proc Natl Acad Sci U S A* **86**, 802-6.

Semenza, G. L. (2000). HIF-1: mediator of physiological and pathophysiological responses to hypoxia. *J Appl Physiol* **88**, 1474-80.

Semenza, G. L., Jiang, B. H., Leung, S. W., Passantino, R., Concordet, J. P., Maire, P. and Giallongo, A. (1996). Hypoxia response elements in the aldolase A, enolase 1, and lactate dehydrogenase A gene promoters contain essential binding sites for hypoxia-inducible factor 1. *J Biol Chem* **271**, 32529-37.

Shweiki, D., Itin, A., Soffer, D. and Keshet, E. (1992). Vascular endothelial growth factor induced by hypoxia may mediate hypoxia-initiated angiogenesis. *Nature* **359**, 843-5.

Spooner, B. S. and Wessells, N. K. (1970). Mammalian lung development: interactions in primordium formation and bronchial morphogenesis. *J Exp Zool* **175**, 445-54.

Sugahara, K., Mason, R. J. and Shannon, J. M. (1998). Effects of soluble factors and extracellular matrix on DNA synthesis and surfactant gene expression in primary cultures of rat alveolar type II cells. *Cell Tissue Res* **291**, 295-303.

Sutherland, D., Samakovlis, C. and Krasnow, M. A. (1996). branchless encodes a Drosophila FGF homolog that controls tracheal cell migration and the pattern of branching. *Cell* **87**, 1091-101.

Taderera, J. V. (1967). Control of lung differentiation in vitro. *Dev Biol* **16**, 489-512.

Wessells, N. K. (1970). Mammalian lung development: interactions in formation and morphogenesis of tracheal buds. *J Exp Zool* **175**, 455-66.

Yamasaki, M., Miyake, A., Tagashira, S. and Itoh, N. (1996). Structure and expression of the rat mRNA encoding a novel member of the fibroblast growth factor family. *J Biol Chem* **271**, 15918-21.

Zhong, H., De Marzo, A. M., Laughner, E., Lim, M., Hilton, D. A., Zagzag, D., Buechler, P., Isaacs, W. B., Semenza, G. L. and Simons, J. W. (1999). Overexpression of hypoxia-inducible factor 1alpha in common human cancers and their metastases. *Cancer Res* **59**, 5830-5.

Zhu, H. and Bunn, H. F. (1999). Oxygen sensing and signaling: impact on the regulation of physiologically important genes. *Respir Physiol* **115**, 239-47.

Zhu, H. and Bunn, H. F. (2001). Signal transduction. How do cells sense oxygen? *Science* **292**, 449-51.